Sonic Boom Considerations in Preliminary Design of Supersonic Aircraft

prepared by

Aurélie Bressollette

Diplôme d'Ingénieur
Option Air Espace
Ecole Centrale Paris, France, 2000

Submitted to the Department of Aeronautics and Astronautics in Partial Fulfillment of the Requirements for the Degree of

Master of Science in Aeronautics and Astronautics
at the
Massachusetts Institute of Technology

February 2002

Copy 2

Signature of Author: ______________________________
Department of Aeronautics and Astronautics
February 1st, 2002

Certified by: ______________________________
Mark Drela
Professor of Aeronautics & Astronautics
Thesis Supervisor

Accepted by: ______________________________
Wallace E. Vander Velde
Professor of Aeronautics and Astronautics
Chair, Committee on Graduate Students

Abstract

This study, conducted at the M.I.T. Gas Turbine Laboratory from September 2000 to December 2001 was focused on design considerations for minimization of the sonic boom. Although there is today a technically sound knowledge of the physics of the boom's generation and propagation, there had been no previous research done on such a specific aircraft. Therefore a deep understanding of sonic boom calculation and minimization had to be conducted first, through review of relevant papers.

The second phase of this study was to discuss how the aircraft's parameters (Mach, altitude, but also length, weight, etc) affected the boom, or more precisely the optimum boom, since no design had been yet drawn before the study was initiated. A boom-minimization computing program and a weight model were used in that scope. Both are outlined in this thesis.

Finally, a first baseline configuration for the Q.S.P. was created. It is briefly described here. These studies could be used as a basis for a more detailed configuration design.

1 INTRODUCTION

Since the development in 1954 of the first operational supersonic fighter, the F100, constant efforts have been undertaken to make routine high-speed flight a reality. The opening of a market for supersonic transportation drove the development of airplanes such as the French-British Concorde. Research programs such as the S.S.T. and the H.S.C.T. lead to major discoveries and technological advances in supersonic transport.

For maximum viability, a long-range supersonic aircraft should have access to overland flight. Yet the F.A.A. has imposed regulations for boom levels that prohibit supersonic overland flight for aircraft developed during the Concorde, SST, and HSCT programs. The purpose of the Q.S.P. project is to develop a high-speed long-range low-boom airplane that will be allowed to fly overland. The approach is to consider the ground boom signature as a fundamental constraint during the design of the configuration and the operating conditions, not as a result of a more relaxed design.

This study, conducted at the M.I.T. Gas Turbine Laboratory from September 2000 to December 2001 was focused on design considerations for minimization of the sonic boom. Although there is today a technically sound knowledge of the physics of the boom's generation and propagation, there had been no previous research done on such a specific aircraft. Therefore a deep understanding of sonic boom calculation and minimization had to be conducted first, through review of relevant papers.

The second phase of this study was to discuss how the aircraft's parameters (Mach, altitude, but also length, weight, etc) affected the boom, or more precisely the *optimum* boom, since no design had been yet drawn before the study was initiated. A boom-minimization computing program and a weight model were used in that scope. Both are outlined in this thesis.

Finally, a first baseline configuration for the Q.S.P. was created. It is briefly described here. These studies could be used as a basis for a more detailed configuration design.

2 THE SONIC BOOM PHENOMENON: CALCULATION, PREDICTION AND MINIMIZATION

With the QSP we aim at designing an airplane based on conventional (or new) practices in accordance with sonic boom minimization concepts. Aerodynamics properties and performances are explored, and the configuration is modified in order to meet compromises between aerodynamics and sonic boom requirements.

The sonic boom concepts do not lead to a single configuration but rather to a set of constraints to be applied to an existing "flexible" design. Therefore, after the sonic boom theory and minimization principles have been thoroughly reviewed, influence of flight conditions and aircraft's parameters on sonic boom will be assessed. This will dictate configuration requirements for a supersonic airplane, which are different from those for an aircraft created independently from sonic boom considerations.

2.1 SONIC BOOM ACCEPTABILITY – HISTORY OF SUPERSONIC RESEARCH – QSP

2.1.1 SONIC BOOM RESEARCH HISTORY

The sonic boom, which in the 1950s was an interesting but little-recognized phenomenon, has since become a major concern in the operation of military airplanes and poses one of the most serious operational problems to be encountered in the development of commercial supersonic transports.

In the late 1950s, the Russians began the development of the TU-144. It first flew in 1968, and then was subject to several redesigns. But after it crashed at an airshow in Paris in 1973, the program was cancelled in 1985. The French-British jointly decided to launch the Concorde program in 1962, and the supersonic airplane made its first flight in 1968. It entered commercial operation in 1976, and stands today as the only commercial operating supersonic transport.

The US had funded research programs on a supersonic transport since the late 1950s. The first important project was the SST in the late 1960s: Boeing Commercial Airplanes was chosen to develop a joint government/industry transport as the result of a design competition. But Congress withdrew government support in 1971. NASA and the industry continued their research in supersonic aerodynamics during the remainder of the 1970s and the early 1980s with the SCAR (Supersonic Cruise Aerodynamics Research), and after 1982 supersonic research was continued only at NASA.

A report in March 1985 by the Aeronautical Policy Review Committee, "National Aeronautical Research & Development Goals: Technology for America's Future", established specific goals in the supersonic flight regimes to enhance this high-payoff technology area. In 1987, a second report stated that the US, in order to maintain leadership in aviation, should develop a program on supersonic transport technology. Increased competition from Japan and Europe lead to the decision for a high-speed research program to develop a second-generation supersonic transport: the High Speed Research (HSR) Program was launched.

In October 1986, feasibility studies by Boeing and Douglas on market, economics, range, Mach number, fuels, payload, and technology needs were conducted. From flight market studies, routes turned out to be predominantly overland. But from the Phase I of the HSR Program (focused on environmental concerns), it came out that industry/government directives included regulations that would affect overland flight: Engine noise around airports should comply with FAR 36-Stage III, the same noise constraints for subsonic aircraft. Overland supersonic flight would only be allowed if the accompanying sonic boom were deemed "acceptable".

Those regulations have become today's environmental constraints, which prohibit overland supersonic flight because of the sonic boom. Environmental studies were conducted in order to evaluate the acceptability of the sonic boom, and regulations imposing a maximum noise level for overland flight have resulted, banning current commercial supersonic aircraft from flying overland. This has greatly affected, for example, the economics of the Concorde. Most routes joining two major international cities are predominantly overland, or include overland flight. It is obvious that the airplane performance in flight duration and probably fuel burn would be enhanced if each route could be entirely flown at supersonic speeds. Therefore, a careful analysis of how the acceptability level for the sonic boom was assessed needed to be conducted, with the goal that the environmental constraint may be overcome.

2.1.2 Acceptability studies

During the 1960s, many flight tests of supersonic vehicles with accompanying boom surveys were held to determine public reaction to the sonic boom. Community surveys (from actual sonic booms produced by supersonic airplanes flying overland) were conducted to assess acceptable noise levels, and effects of booms on both people and structures.

Overpressure values in pounds per square foot (the amount of pressure above normal atmospheric pressure, 2,116 psf) were used to measure sonic booms:

- At 1 psf of overpressure, no damage to structures occurs.
- 1 to 2 psf of overpressure occur at ground level from aircraft flying at supersonic speeds at normal operating altitudes. Overpressure above 1.5 psf is irritating to people.
- At 2 to 5 psf some minor damage can occur to structures.
- As overpressure increases, the chance of structural damage increases. Structures in good condition can withstand overpressures of up to 11 psf.
- 20 to 144 psf are experienced at ground level when aircraft fly at supersonic speeds at altitudes of less than 100 feet. Such levels of overpressure have been experienced by humans without injury.
- At 720 psf damage to eardrums results. At 2160 psf lung damage occurs.

At Langley Space Center, laboratory studies on subjective response to sonic boom (by using simulated sonic boom's methods) were held. Indications resulted that bow shock level and shock rise time (shocks creating the sonic boom phenomenon) are both very important factors in the loudness of a sonic boom signature on the ground.

These results gave rise to a real concern on sonic boom in operational studies for supersonic aircraft. The QSP Project launched by DARPA strongly reflects that critical issue.

2.1.3 THE QSP

The Quiet Supersonic Platform (QSP) program is directed towards development and validation of critical technology for long-range advanced supersonic aircraft with substantially reduced sonic boom, reduced takeoff and landing noise, and increased efficiency relative to current-technology supersonic aircraft.

The program is designed to motivate approaches to sonic boom reduction that bypass incremental "business as usual" approach and is focused on the validation of multiple new and innovative "breakthrough" technologies for noise reduction that can ultimately be integrated into an efficient quiet supersonic vehicle. Given the objective of validating an approach to sonic boom mitigation, the single QSP requirement under RA 00-48 is the reduction of sonic boom ground signature initial shock strengths to an amplitude no greater than 0.3 psf.

This value represents a real challenge, since all the other commercial supersonic airplanes fly with higher values:

- 0.8 psf for the F-104 (1954) at Mach 1.93 and 48,000 feet.
- 0.9 psf for the SR-71 (1966) at Mach 3 and 80,000 feet.
- 1.25 psf for the Space Shuttle (1981) at Mach 1.5 and 60,000 feet during landing approach.
- 1.94 psf for the Concorde SST (1976) at Mach 2 and 52,000 feet.

But once again, the 0.3 psf value will allow overland flight, significantly increasing the aircraft's efficiency in terms of range and duration of flight.

This program is intended to benefit both military aircraft and supersonic business jet developments. Indeed, the Pentagon's current defense review will likely call for improvements in long-range precision-strike forces. Supersonic-cruise aircraft could be invaluable for intercontinental missions, avoiding the marathon 30-hour sorties that the B-2 flew in the Kosovo campaign. Supersonic aircraft could deliver their first attacks more quickly and fly more missions in the same time span. As for supersonic business jets, their development could be boosted by new efficient concepts for sonic boom reduction, since this would also open them to the highly valuable overland space.

The vision of the DARPA QSP program is to foster the development of new technologies sufficient to mitigate sonic boom to the point that unrestricted supersonic flight over land is possible.

2.2 SONIC BOOM PHENOMENON: PREDICTION AND CALCULATION

The sonic boom has emerged at the forefront of the problems confronting the advancement of worldwide transportation systems. In this period, the combined efforts of scientists and engineers in this country and abroad have replaced the former uncertainties and misconceptions surrounding the nature of the sonic boom with a technically sound knowledge of the physics of its generation and propagation. There is now a general understanding of the way in which an airplane's shape, size, and operating conditions affect the generation of the sonic boom, and of the way in which atmospheric conditions and airplane flight-path variations affect the propagation.

2.2.1 THE PHENOMENON

When an airplane travels through the air, it causes pressure disturbances that give rise to sound waves. Those waves propagate away from the aircraft at the speed of sound.

As the aircraft travels faster than the speed of sound, the aircraft travels faster than the sound it emits. The airplane actually moves ahead and away from the sound it emits at a speed equal to the speed of the aircraft minus the speed of sound. This creates pressure disturbances in the air resulting in the formation of shock waves. Shock waves reaching the ground produce sonic booms. The phenomenon has been represented on Figure 2.1. Figure 2.2 reveals the disturbances as the aircraft passes through the air at a speed greater than the sound speed.

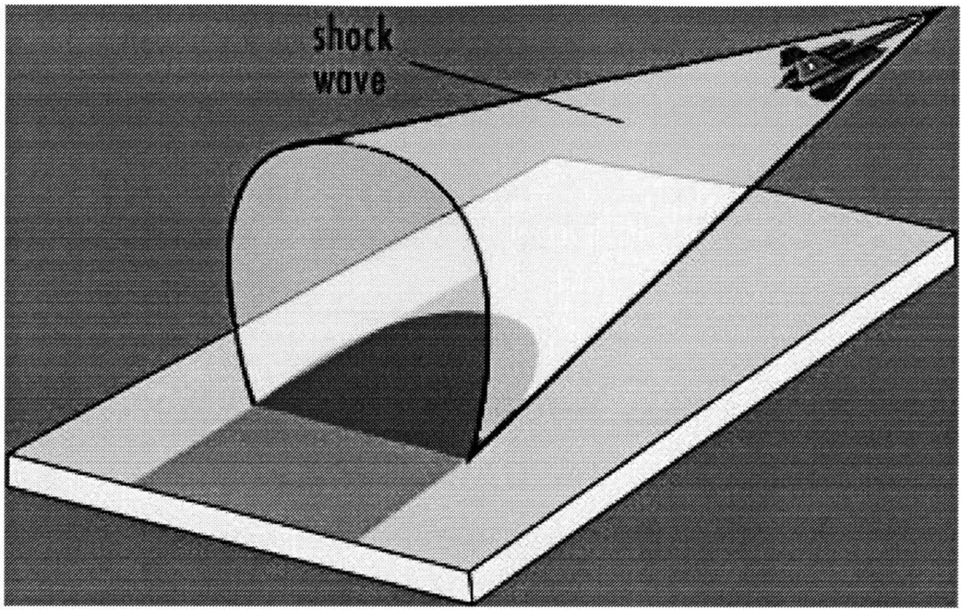

Figure 2.1: Shock waves and sonic boom generation

Figure 2.2: Visualization of disturbances generation

A typical airplane generates two main shock waves: one at the nose and one at the tail. When these waves, along with the aircraft's secondary waves, propagate to the ground, they tend to coalesce with each other, giving rise to two main pressure pulse changes: on is an abrupt compression above atmospheric pressure, followed by a rapid decompression below atmospheric pressure, the other is a final recompression to atmospheric pressure. To an observer on the ground, the resulting pressure pulse changes appear to be N-shaped. The total change takes place in 1/10 second or less and is felt and heard as a double jolt or boom. Figure 2.3 shows the resulting "N-wave" on the ground.

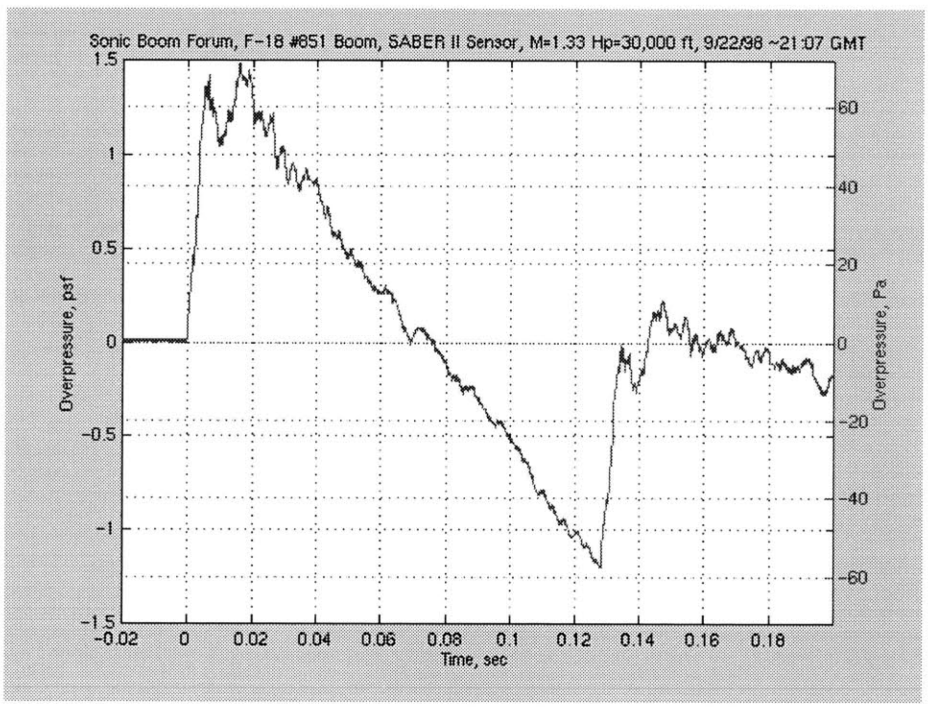

Figure 2.3: Recording of an N-wave at ground level

The strength of the shock waves and the boom is characterized by the associated overpressures. As we move further from the aircraft, the intensity of these overpressures tends to decrease because of attenuation during propagation through the atmosphere. This allows definition of three distinct regions around the airplane: the near field, the mid field, and the far field.

The near field pressure distribution is given by analysis of aircraft's shape, and each component affects the signature both independently and by interacting with every other component. The mid field represents the region further from the aircraft, where waves have begun to coalesce, so that aircraft's components' influence on pressure distribution is reduced, but where the signature has not yet acquired its final N-shape. This typical pressure signature is reached in the far field, where all waves have coalesced, and where moving further away from the aircraft leads to reduction of overpressures only, and not to modification of signature shape (Figure 2.4).

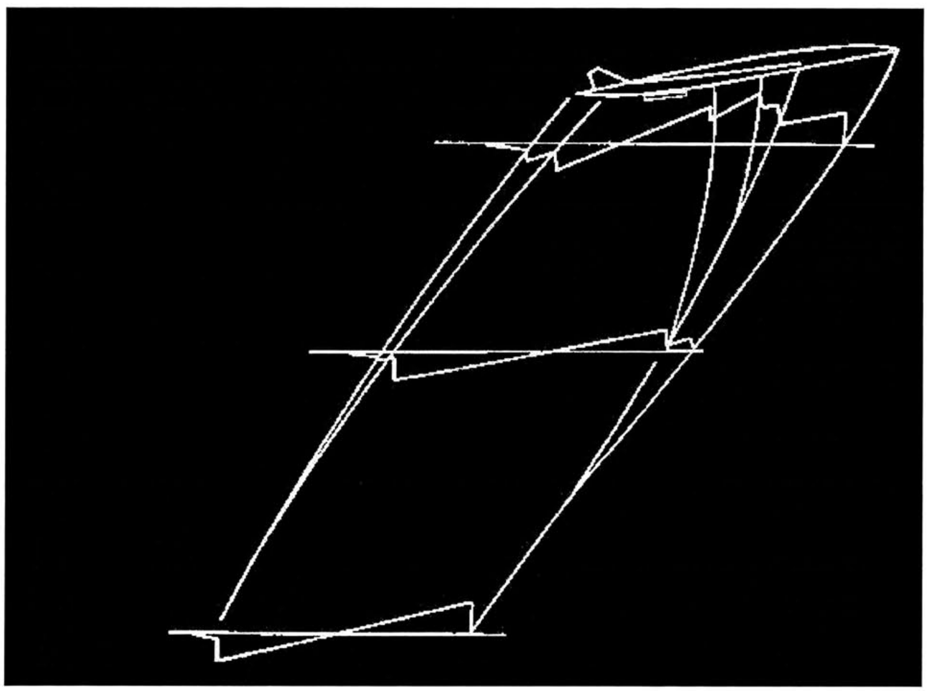

Figure 2.4: Near, mid and far fields

Typically, as we move away from the airplane ground track, overpressures tend to decrease and signature length to increase inside the Mach cone, where the pressure disturbances created by the airplane are confined. Signature changes within this region are due not only to the increase of propagation distance off track, but also to the decreasing influence of airplane lift and weight away from a vertical plane. This is the reason why it has been admitted for a long time that changes in airplane configuration offered few opportunities for sonic boom reduction.

However, even if the N-wave shape appears like the necessary shape of the boom that would be recorded at ground level for any airplane, it needs not to be so: indeed, McLean first observed in 1965 that for supersonic aircraft of practical length, the midfield region in a homogeneous atmosphere could extend several hundred body lengths. In 1967, Hayes pointed out that according to this result for a homogeneous atmosphere, the midfield effects should persist indefinitely below the aircraft in the real atmosphere. This phenomenon is called the "freezing" of the overpressure signature. Stuff later extended this result to a stratified atmosphere.

The Hayes analysis also showed that the "freezing" phenomenon is more significant in the actual non-uniform atmosphere (where a wave develops more gradually) than it is in a uniform atmosphere. It therefore means that near-field minimization concepts become of even greater significance.

The aircraft can also be such that the signature on the ground will turn as the far-field N-wave. Near the airplane the pressure signatures are characteristically complex and contain multiple shocks. Under some conditions, typically for large slender airplanes in the transonic speed range, these more complex signatures will persist to ground level.

Therefore the influence of airplane's configuration on the pressure signature becomes more relevant, whether the signature recorded on the ground is the N-wave or not. Near-field and mid-field studies and the way aircraft's shape affects them offer more opportunities for sonic boom reduction. Thus it is appropriate that calculation techniques allow consideration of the more general near-field or mid-field signature rather than being restricted by simplifying far-field assumptions, and then take into account the atmosphere's properties for study of disturbances' propagation.

2.2.2 NEAR-FIELD CALCULATION

Sonic boom studies were initiated in the 1950s by Whitham, who first formulated a theory for calculating the near-field pressure distributions around a supersonic body. There are two distinct sources of disturbances: one due to lift, and one due to the aircraft's volume.

From airplane's shape and flight conditions, Hayes used area-rule concepts to determine the equivalent area distribution due to lift, as well as the area distribution formed by the airplane volume. This process leads to the equivalent body of revolution geometry, and from that to the Whitham F-function, which links body geometry and pressure field near the airplane.

The F-function method is based on the linearized theory of supersonic flow, which accounts for disturbances close to the body. It was used by Whitham to determine pressure signature in the near field. Signature at any propagation distance is obtained via corrections to the F-function, corresponding to a corrected linearized theory.

2.2.2.1 Whitham's F-function based on supersonic linearized theory

The most direct way to calculate pressure disturbances from a given configuration causing the boom on the ground would be to use the method of characteristics and finite difference techniques. The process would start by taking each part of the airplane and calculate the independent pressure disturbances it creates. The next step would be to correct them by accounting for the interaction of each distribution with every other one. The propagation path of each distribution would then be determined, allowing for the alteration of paths by every other disturbance. Finally, the signature would be calculated by accounting for coalescence of all the distributions and the formation of shocks.

This method is the most logical and rigorous one, but turns out to be very hard to implement when dealing with the complex case of a complete airplane configuration. Also, each change in design could only be analyzed by rerunning the entire procedure, implying long computing times and high costs.

Instead, we turn towards the work done by Whitham in the 1950s on sonic boom calculation (and prediction), which is based on the linearized theory of supersonic flow.

$$\frac{p(x,r,\theta)}{\gamma P_* M^2} = \frac{1}{(2\beta r)^{\frac{1}{2}}} \frac{1}{2\pi} \int_0^{x-\beta r} \frac{A''(\xi;\theta)}{(x-\beta r-\xi)^{\frac{1}{2}}} d\xi \qquad (2.1.a)$$

$$F(y) = \frac{1}{2\pi} \int_0^{y} \frac{A''(x)}{(y-x)^{\frac{1}{2}}} dx \qquad (2.1.b)$$

However, linearized theory does not provide a consistent first-order description of the flow-field far from the aircraft: this is the reason why the F-function is distorted to calculate propagation through the atmosphere.
A first-order theory computes values that are in the same order as the slenderness ratio of the aircraft (the "thickness" of the aircraft divided by its length). A typical value of slenderness ratio is 1/20. In order to correct the first-order theory, second-order terms in the near-field pressure distributions that will affect the first-order terms far from the aircraft need to be taken into account. The work done by Seebass (Reference: Sonic Boom Theory 1969) in 1969 provides means of correcting the theory for the case of steady flight in an atmosphere without winds.

2.2.3 FAR FIELD: PROPAGATION THROUGH THE ATMOSPHERE

Now that we have given means for obtaining the pressure distributions in the vicinity of the airplane, a way of obtaining the aircraft's signature far from the body needs to be assessed, since the sonic boom is precisely a far-field phenomenon. The Whitham F-function should be used as a starting point for determining the boom on the ground after propagation of the disturbances through the atmosphere.

Typically, as underlined earlier, when the aircraft's shock waves make their way to the ground, they tend to coalesce with one another, and the 2 main shocks (the front one and the rear one) remain the most dominant ones, leading to a far-field "N-wave" signature: an abrupt rise in pressure (above the atmosphere's normal steady level) followed by a decrease and an abrupt rise back to the original level. Because of this coalescence phenomenon, the aircraft's components do not exert a very strong

influence on the pressure signature's shape since only the front and rear shocks remain dominant.
However, as already pointed out, the far-field signature need not be always the typical N-wave shape. Because of the "freezing" phenomenon described earlier, the mid-field can persist to the ground. In that case, the boom minimization process can be greatly enhanced by thoroughly studying the airplane's components' configuration, since the aircraft's shape does affect the mid-field's signature shape. This means that a careful review of how changes in configuration will influence the near-field pressure distributions and how they will propagate to the mid-field can lead to serious sonic boom reduction.

Hayes, George and Seebass were the first to study the propagation of waves through a homogeneous atmosphere. In the real atmosphere, temperature gradients, winds and other disturbing factors will affect the resulted signature on the ground: normal steady-state atmospheric properties are responsible for overpressure magnitudes and distributions differing from the uniform atmosphere situation, where N-waves signatures are considered to represent nominal or average conditions. Atmospheric non-uniformities or distortions introduce significant and sometimes drastic variations from this form. In the presence of atmosphere turbulence, the waveforms may display either sharp pikes or considerable rounding at shock locations.

There is now a general understanding of the way in which atmospheric conditions and airplane flight-path variations affect the propagation of the boom after generation near the aircraft's body. It is true that calculated overpressures are nominal and thus do not account for small-scale atmosphere variability. But this does not restrict practical use of the prediction methods, since nominal values provide a point of reference about which perturbations due to atmospheric factors can be estimated on the basis of statistical data obtained in flight-test programs.

From those theories, propagation codes have been created in order to assess the airplane's signature on the ground from configuration's data. The inputs differ from one program to another:

- The ARAP code, developed by Hayes (Ref. 3): it computes the Whitham F-function and predicts how the pressure signature propagates through the atmosphere to the ground.
- The NFBOOM code (Ref. 8).

Many in-flight experiments have been conducted in order to assess airplane's signature on the ground after propagation through the atmosphere. Since these studies were run for specific aircraft in real conditions, the results can hardly be used for general considerations on sonic boom propagation through the atmosphere. However, a list of relevant articles is available to the reader at the end of this thesis.

2.3 SONIC BOOM MINIMIZATION

It has been stressed that the sonic boom stands as one of the major concerns in the design of a supersonic airplane, especially when it is intended for overland flight. The ability to predict the boom can now be linked to the design process. However, it will be explained that one cannot simply design an airplane from boom minimization considerations (otherwise there would be only one solution design already known by anyone). Indeed, there is an infinite number of configurations that can meet minimization's requirements, for a given set of flight parameters. Therefore minimization principles will first be clearly stated. Then, interactions between those considerations and the design process will be emphasized, for this will provide concrete means of implementing the sonic boom theory to the QSP design.

2.3.1 THEORETICAL APPROACH

The previously developed principles of sonic boom prediction (calculation and propagation) form the base for sonic boom minimization. The key point in this theory is the Whitham F-function, which links the airplane's configuration to its pressure signature.

It should be stressed that there is no well-established set of nominal pressure signature characteristics that would commonly be accepted as a solution to the problem: what is a minimum sonic boom? Little is known of the relative importance of the various signature parameters, such as peak overpressure, shock strength, impulse, rise time, and so forth.

Shock strength is believed to be the controlling factor to outdoor annoyance; but for the far more common indoor exposure situation, noise and annoyance may be related to signature impulse and duration and other factors as well. For structural response and building damage criteria, the problem is equally complex. Goal signatures for this study, however, should be based on DARPA requirements for the QSP of overpressures not exceeding 0.3psf: peak overpressure is thus the driving factor.

As it can also be assumed that one of the most annoying features of the sonic boom, at least as it experienced outdoors, is due to the presence of shock waves in the pressure signature, we turn to the question of whether it is indeed possible to design practical aircraft with overpressure signatures that do not contain shock waves. Seebass pointed out that it is hypothetically possible to completely eliminate both shock waves from the pressure signature. This implies length requirements, given certain aircraft's parameters like Mach number and weight. However, this is overly optimistic, since the length required is beyond our present structural capability. Thus it should be accepted that the pressure signature *will* include shock waves.

Now, when a signature with shocks is prescribed, these characteristic lines considered to be absorbed in the shock are not uniquely related to a given F-function. In other words, there are an infinite number of F-functions that will eventually lead (after propagation through the atmosphere) to the same ground signature. However, other studies show that the F-functions for the lower bound of an N-wave and for the lower bound of the bow shock in a mid-field signature can be determined, and lead to the form of the minimizing F-function, as assumed by Seebass and George for the entire signature.
As underlined earlier, because of non-uniqueness properties other F-functions may lead to the same optimized signature. Yet this particular form is linked to the optimized sonic boom, in the sense that for given airplane's and flight's parameters, there cannot be any reduction in sonic boom once the aircraft's F-function is similar to that particular form.

Christine M. Darden (Ref. 10) used this theory to develop a code known as the Seeb code: the computer program calculates both the minimizing-pressure signature and the required equivalent-area distribution for a given cruise Mach number, altitude, and aircraft length and weight. Using area distributions from this program as constraints for the design of 3 low-boom wind-tunnel models, this minimization procedure has been verified experimentally.

The theory underlining the code uses the described F-function form, which allows minimization of various signature parameters. In mathematical terms, it may be expressed as:

$$F(y) = 2yH/y_f \qquad 0 \le y \le y_f/2 \qquad (2.2.a)$$

$$F(y) = C(2y/y_f - 1) - H(2y/y_f - 1) \qquad y_f/2 \le y \le y_f \qquad (2.2.b)$$

$$F(y) = B(y - y_f) + C \qquad y_f \le y \le \lambda \qquad (2.2.c)$$

$$F(y) = B(y - y_f) - D \qquad \lambda \le y \le l \qquad (2.2.d)$$

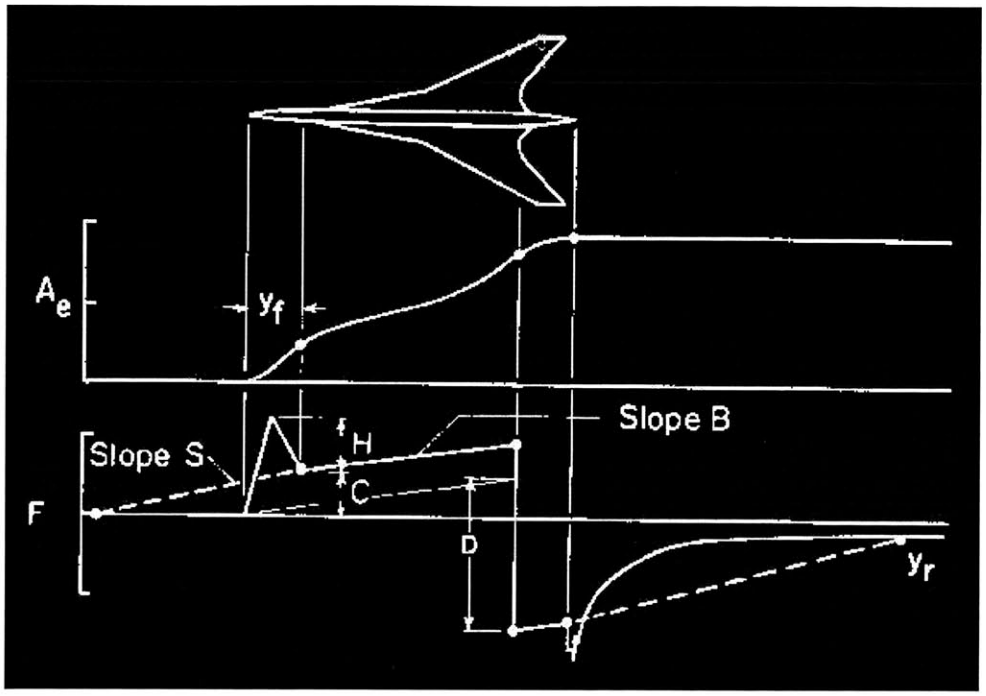

Figure 2.5: F-function and Equivalent Area Distribution, with parameters

y_f corresponds to the "length" of the nose. H, B, C, D and λ are unknown coefficients which are determined by given cruise conditions, nose length, prescribed ratio of bow to rear shock, and by the signature parameters to be minimized. As it has been assumed earlier that overpressure level should be the major concern, flat-topped N-wave signatures with minimum overpressures should be the ones considered and aimed at. For these signatures and for minimized overpressures, B should be 0.

2.3.2 REQUIREMENTS ON AIRCRAFT DESIGN

Now it should be recalled that the F-function represents the shape characteristics of the pressure signature and is defined in terms of equivalent area distribution as:

$$F(y) = \frac{1}{2\pi}\int_0^y \frac{A_e''}{(y-\xi)^{1/2}}\,d\xi \tag{2.3}$$

where y is the longitudinal coordinate along the aircraft's fuselage.
Crucial to this minimization technique is the fact that equation (2.3) is an Abel integral equation which may be inverted to give the function A_e (the airplane's equivalent area distribution, the "Mach" slices) in terms of the F-function. When this function is evaluated at l the result is:

$$A_e(l) = 4\int_0^l F(y)(l-y)^{1/2}\,dy \tag{2.4}$$

Upon substituting the minimizing form of the F-function into equation (3) and integrating, the following equation for the development of cross-sectional area is obtained:

$$A_e(x) = \frac{32}{15}\frac{H}{Yf}x^{5/2}$$

$$+\delta(x-Y_f)\frac{8}{15}\left(x-\frac{Y_f}{2}\right)^{3/2}\left[\left(\frac{3Y_f}{2}+2x\right)\left(\frac{1}{Y_f}\right)(2C-4H)+5(2H-C)\right]$$

$$+\delta(x-Y_f)4(x-Y_f)^{3/2}\left[\frac{2C}{Y_f}\left(-\frac{2}{15}\right)(3Y_f+2x)+\frac{2}{3}C+\frac{4}{15}\frac{H}{Y_f}(3Y_f+2x)-\frac{4}{3}H+\frac{2}{15}B(3Y_f+2x)-\frac{2}{3}BY_f+\frac{2}{3}C\right]$$

$$-\delta(x-Y_f)\frac{8}{3}(x-\lambda)^{3/2}(C+D) \tag{2.5}$$

where $\delta(x-l)$ is the Heaviside unit step function. As overpressure is the chosen leading factor in the boom minimization process used here, B is 0, thus:

$$A_e(x) = \frac{32}{15}\frac{H}{Yf}x^{5/2}$$

$$+\delta(x-Y_f)\frac{8}{15}\left(x-\frac{Y_f}{2}\right)^{3/2}\left[\left(\frac{3Y_f}{2}+2x\right)\left(\frac{1}{Y_f}\right)(2C-4H)+5(2H-C)\right]$$

$$+\delta(x-Y_f)4(x-Y_f)^{3/2}\left[\frac{2C}{Y_f}\left(-\frac{2}{15}\right)(3Y_f+2x)+\frac{2}{3}C+\frac{4}{15}\frac{H}{Y_f}(3Y_f+2x)-\frac{4}{3}H+\frac{2}{3}C\right]$$

$$-\delta(x-Y_f)\frac{8}{3}(x-\lambda)^{3/2}(C+D) \qquad (2.6)$$

What equation (2.6) reflects is the "path to follow" in order to obtain a minimum overpressure level on the ground, given cruise and aircraft parameters. Once these parameters have been specified, they determine the unknown H, C, D and λ, and thus $A_e(x)$. Then, efforts should be concentrated on trying to match the proposed aircraft's equivalent area distribution with this $A_e(x)$, which is the one leading to an optimum pressure signature for the defined aircraft and cruise parameters.

The process has been summarized in Figure 2.6:

Minimizing Form of F-function $F(y)$

with parameters

Minimizing $A_e(x) = 4\int_0^x F(y)\sqrt{(l-y)}.dy$

with parameters

Mach, Weight, Length, Altitude

Values of H, C, D and λ

Minimizing $A_e(x)$ determined

Figure 2.6: Determination of design requirements for minimization

Now the question is how H, C, D and λ can be determined once cruise Mach number and altitude, and aircraft's length and weight have been specified.

According to Darden's theory, the minimization process used in the Seeb codes is based on 5 requirements/constraints:

1 – If the effects of the aircraft wake and engine exhaust are neglected, and, if the aircraft cross-section area is zero at its base, then **the area at l is entirely due to cruise lift**, or

$$A_e(l) = \frac{W}{\rho u^2} \tag{2.7}$$

where W is the airplane weight, and u its speed.
Therefore calculations are made with **constant lift**.

2 – The front area balance must occur at $y = y_f$ where y_f is the first point at which $F(y) = C$ (see minimizing form of F):

$$\int_0^{y_f} F(y)dy = G = \frac{\alpha_{y_f}}{2}C \tag{2.8}$$

3 – The rear area balance must occur between l and y_r (2nd intersection point of the rear area balancing line with $F(y)$):

$$\int_l^{y_r} F(y)dy = \frac{1}{2}\left[B(l - y_f) - D + F(y_r)\right](y_r - l) \tag{2.9}$$

4 – The constraint on the ratio of shocks is given by:

$$\frac{P_f}{P_r} = \frac{C}{D - B(l - y_f) + F(y_r)} \tag{2.10}$$

5 – To ensure that y_r is an intersection point of $F(y)$ and the balancing line,

$$F(y_r) = S(y_r - l) + B(l - y_f) - D \tag{2.11}$$

2.3.3 Applying the process to the QSP

The previously described minimization theory constitutes the baseline for the Seeb code, which was used for this study. Thanks to this fast and reliable program, one has access to the required area distribution to minimize overpressure level on the ground once the aircraft's cruise Mach number and altitude, and length and weight have been set. The Seeb code thus constitutes a very powerful tool for any team of designers who have already conceived a first proposed configuration for an airplane whose cruise parameters have been set through mission requirements, and who are willing to add changes to their design in order to minimize the sonic boom of their aircraft.

However, for the QSP, no specific Mach number and especially no cruise altitude had been defined yet, and no configuration had been proposed. It was therefore essential to be able to analyze the influence of each of these parameters on the *optimized* sonic boom, since at least one constraint imposed by DARPA was clearly set: the overpressure on the ground should not exceed 0.3psf.

In the next part of this paper, independent influence of length, weight, Mach number and altitude on optimized sonic boom will be assessed. This analysis was intended to lead to a choice of cruise parameters (the major concern being altitude), and of imposed (but realistic) aircraft's length and weight.

3 INFLUENCE OF FLIGHT'S PARAMETERS ON OPTIMIZED SONIC BOOM

This study has two scopes: the first one is to assess the influence of each parameter on the *optimized* sonic boom. The word "optimized" is crucial here: we are not, for example, analyzing the change in ground signature while the aircraft rises up to its cruise altitude. We want to determine how each *fixed* parameter affects the value of the *best achievable* (thus the minimum) overpressure level. Thus different altitudes represent different possible *cruise* altitudes from which one will be eventually chosen for the mission. The corresponding overpressure (given by the Seeb code) will be the *optimized* value for that particular cruise altitude.

The second scope of the study presented here is to provide some elements of decision for the considered QSP parameters (Mach, altitude, length and weight).
In order to consider only realistic sets of parameters (altitude, length and weight (and in a certain extent, Mach) are logically linked), a weight buildup has been set up in. Description and results for this model are reviewed.

The main inputs for the Seeb code are considered to be the aircraft's parameters:

- The cruise Mach number;
- The cruise altitude;
- The aircraft's overall length;
- The aircraft's gross take-off weight.

Other options are also available, like optimizing the length given a desired sonic boom overpressure (values between 0.5psf and 1.0psf), or changing the nose bluntness (the corresponding parameter being y_f). The first option has not been considered since the targeted maximum overpressure value is 0.3psf, and the second option is more likely to be used for design corrections, not for a first overview of how each parameter will affect the boom performance of the aircraft, and provides very little help for deciding which set of parameters will eventually be used.

The outputs to be considered are the following:

- The optimized sonic boom, given the aircraft's parameters (thus the lowest sonic boom level the aircraft can produce thanks to an appropriate shaping);
- The required effective area distribution (in order to achieve the optimized sonic boom level);
- The corresponding F-function.

Again, other outputs are available, but they present little (if none) relevance to the study conducted.

It should be recalled that the decision was taken to define "minimize sonic boom" as the equivalent of "minimize overpressure", which implies considering only flat-topped signatures (the ones aimed at). This is essential to point out this characteristic of the work presented, since depending on which values is minimized (overpressure, initial shock or impulse) the differences in the resulting signature shapes are quite significant.

3.1 Independent Influence of Parameters by Using the Seeb Code

To keep the results in perspective, the emphasis of this study is focused primarily on the trends in optimized overpressure. By analyzing and evaluating these trends, the relative importance of each study parameter and its effect on the overpressure levels can be determined. These results will provide guidance later in this paper in determining the conditions under which the QSP may be best operated and shaped for low boom.

3.1.1 Mach Number

The study was conducted for Mach number between 1.7 and 3.0. All other parameters (as inputs to the Seeb program) were kept constant, at the following values:

- Length = 160ft;
- Weight = 100,000lbs (maximum gross take-off weight imposed by DARPA);
- Altitude = 50,000ft.

Figure 3.1 shows the resulting optimized overpressure levels for each Mach number (again, each point corresponds to one single and independent aircraft shaped for minimum (best achievable) boom level):

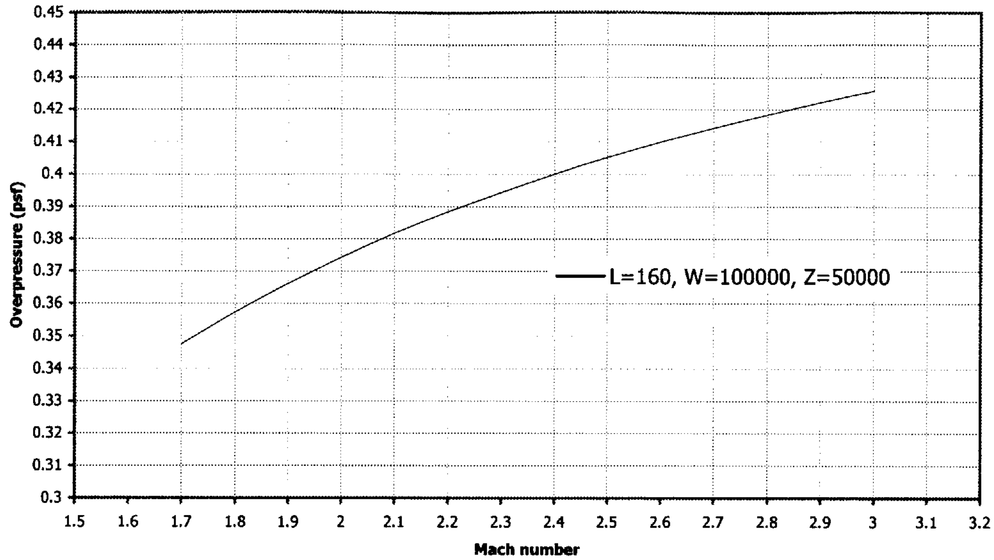

Figure 3.1: Influence of Mach number on optimized overpressure level

An increase in Mach number obviously did not result in a significant increase in overpressure. As highlighted earlier, caution should be taken here though, since all other parameters (especially cruise altitude) were kept constant whereas an increase in cruise Mach number would normally be linked to an increase in cruise altitude, in realistic conditions. However this plot still allows the statement that Mach number alone does not affect optimized sonic boom level significantly.

3.1.2 LENGTH

In order to assess the influence of aircraft's length on overpressure level, the following values were used for the other parameters kept constant:

- Mach number = 2.3 (as imposed by DARPA for the QSP);
- Weight = 100,000lbs;
- Altitude = 50,000ft.

The values considered for length ranged from 80ft to 180ft.
Figure 3.2 summarizes the results obtained:

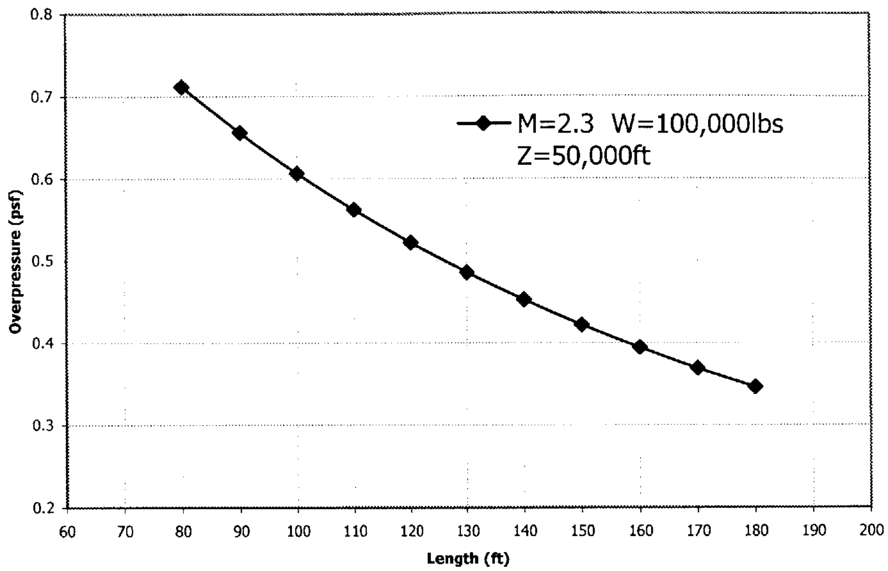

Figure 3.2: Influence of length on optimized overpressure

As already pointed out, this is not very realistic since weight should change with length. But once again, the *independent* influence of length is investigated here, in order to provide a better idea of how each design parameters individually affects the best achievable overpressure level.

The results clearly demonstrates that the longer and slender the airplane, the lower the resulting sonic boom on the ground. However designing a long and slender aircraft is a typical structural problem, and it has been pointed out earlier that this corresponds to a limit which makes it impossible with today's technology to design an airplane meeting length requirements for the phenomenon of "freezing" (when the signature remains the mid-field signature to the ground). Therefore trends studies should be conducted and trade-offs should be established before any decision can be taken upon aircraft's length.

3.1.3 WEIGHT

A study similar to the previous one was conducted for the effect of aircraft's weight on the optimized overpressure. The following values for the fixed design parameters were used:

- Mach number: 2.3;
- Length: 120ft;
- Cruise altitude: 50,000ft.

Figure 3.3 shows the results obtained after running the Seeb code for weight values ranging from 50,000lbs to 110,000lbs:

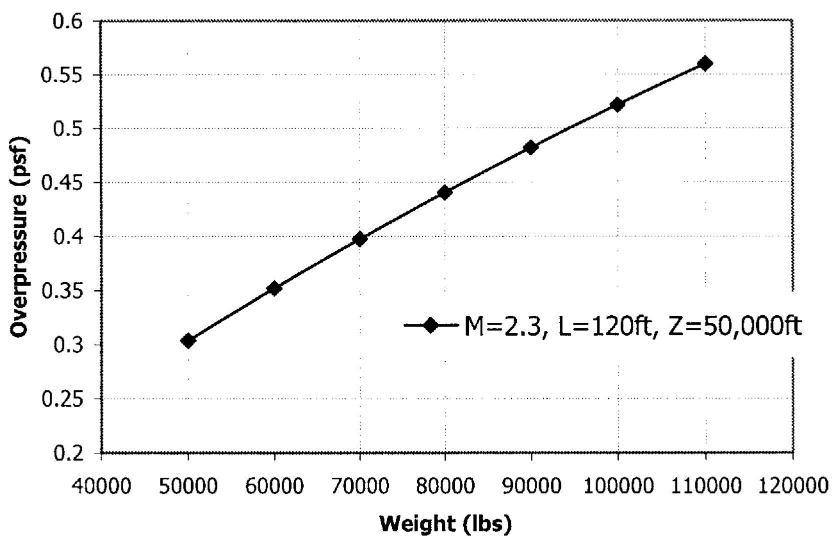

Figure 3.3: Influence of weight on optimized overpressure

Clearly, the heavier the aircraft, the higher the resulting sonic boom. Also, Needleman and Mack found that by reducing the cruise weight, the altitude range available in the design envelope for generation of mid-field signature would increase. And as seen earlier, setting up the cruise altitude in such a way that the signature recorded on the ground is the mid-field signature is critical in reducing the resulting overpressure level (to avoid the "jump" described by Needleman and Mack).

Now we have seen earlier that in order to achieve a low boom the aircraft should be as long and slender as possible. This deviation from a standard supersonic design will necessarily lead to consequently increased weight, and thus higher overpressure level. In this scope a powerful and reliable method for linking length and weight in a realistic approach is required in order to reach a good compromise between these two contradicting trends. The weight model implemented for this study will be presented later.

First, we need to assess how cruise altitude will affect the optimized level of overpressure, since atmospheric properties (the environment in which the airplane will operate) will strongly influence the choice of aircraft's size, i.e. length and weight.

3.1.4 Altitude

Needleman and Mack (Ref. 9) conducted a study on sonic boom minimization that offers very interesting results: two conceptual Mach 2.0 configurations, originally designed to meet similar mission criteria, were analyzed for a representative range of weights, altitudes, and Mach numbers.

The result on which attention has been focused is the influence of altitude on overpressure signature on the ground. For both configurations and for each weight and Mach number, Needleman and Mack observed the same phenomenon: first the overpressure continually decreased as altitude increased, due to atmospheric attenuation. This trend continued until the signature reached an altitude where the intermediate shocks coalesced with the forward shocks. At coalescence, the overpressure jumped to a significantly higher level after which it once again began to slowly decrease, again due to attenuation. This transition actually marked the transition from a mid-field multi-shock signature to a far-field N-wave signature.

Common sense says that the higher the altitude, the lower the boom, because of attenuation. However this study clearly reveals that care should be taken about the cruise altitude: it should not exceed the value where the resulting overpressure on the ground would jump to a much higher level. Also, changing properties of the atmosphere with increasing altitude should be carefully taken into consideration. All these assessments highlight the importance of cruise altitude as a major factor in sonic boom minimization.

However, once again the altitude study that was conducted by Needleman and Mack was based on 2 *existing* configurations: even if it clearly demonstrates the importance of cruise altitude choice, it does not say how this parameter independently affects the *optimized* overpressure level. To investigate this influence, several runs of the Seeb program were conducted, with cruise altitude values ranging from 10,000ft to 90,000ft. In order to prove that the individual effect of altitude does not depend on the chosen values for length and weight, four sets of aircraft's parameters were used:

- Length L=120ft, Weight W=80,000lbs;
- Length L=120ft, Weight W=100,000lbs;

- Length L=160ft, Weight W=80,000lbs;
- Length L=160ft, Weight W=100,000lbs.

(100,000lbs being the value considered by DARPA as the maximum gross take-off weight for the QSP).

The Mach number was kept constant at 2.3 (again, as imposed by DARPA).

Figure 3.4 sums up the values obtained for optimized overpressure level:

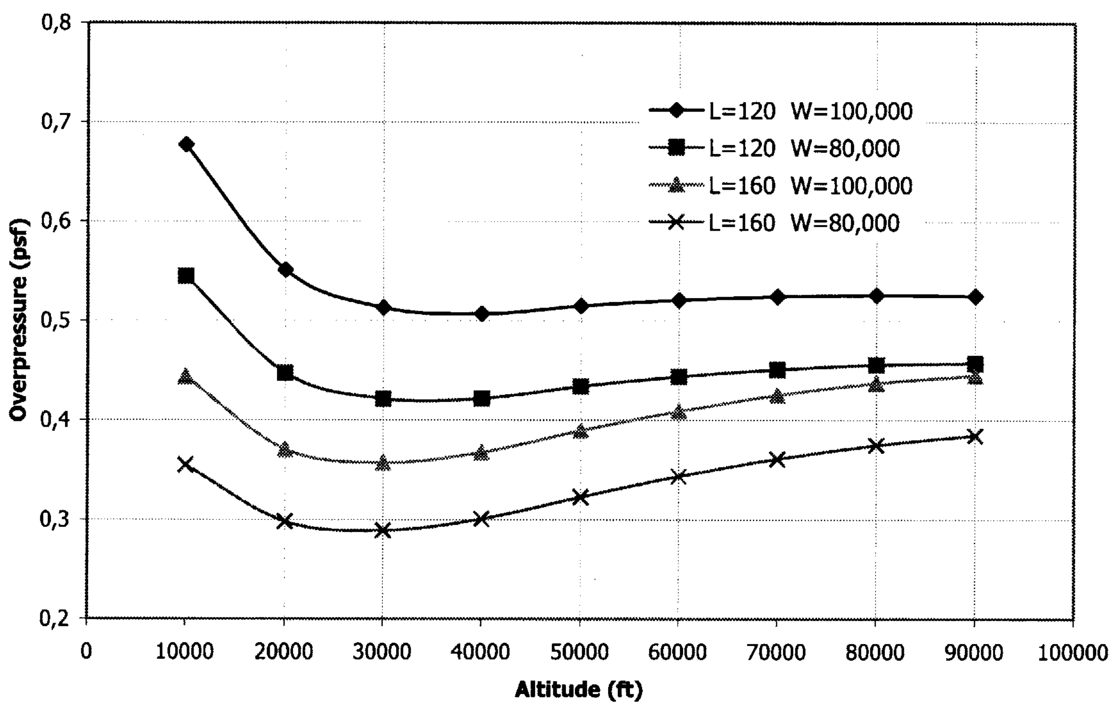

Figure 3.4: Influence of cruise altitude on optimized overpressure

Once again, each point on this graph corresponds to an independent configuration for which a set of parameters (Mach, Length, Weight and Cruise Altitude) has been specified and for which the boom has been minimized. It should not be seen as if one curve was for one airplane climbing in altitude.

The results obtained lead to the following remarks:

- The trends vs. length and weight, as demonstrated earlier, are verified on this diagram: the longer and the lighter the aircraft, the lower the boom, whatever the cruise altitude.
- Each curve reaches a minimum, which means: there exists a "best" cruise altitude for given length and weight.

Caution should be taken regarding this last idea. On one curve of Figure 3.4, length and weight are kept constant, whereas the cruise altitude is increased/decreased. This cannot be realistic, since an airplane designed to fly at higher altitude should be larger than if it was meant to fly lower. Indeed, the atmosphere becoming thinner at higher altitude, the dynamic pressure decreases, and so the required wing area increases. Therefore, one cannot consider the length and weight to remain constant if the cruise altitude is changed.

The "realistic" curve would be composed of points from these different curves, length and weight increasing with cruise altitude. How the aircraft's size is linked to its designed flight altitude is at the core of the problem for optimizing cruise altitude. The other major issue is to link the length of the airplane to its weight.

These two issues are still more critical considering the conflicts between length's and weight's influence on sonic boom level: as cruise altitude increases, the aircraft must be larger. Thus length increases, but so does weight. As the optimized sonic boom level rises with weight but diminishes with length, assessing the resulting sonic boom when cruise altitude is increased requires a more detailed analysis of how length and weight are linked.

We have a sense of how aircraft's size is related to the atmospheric altitude at which the aircraft will be flying: it comes directly from aerodynamics considerations: the lift of the aircraft must equal its weight. Or in other words, its wing area should support its weight.

Once the airplane's aerodynamics (C_L, L/D) are fixed, required aircraft's size scaling can be directly related to cruise altitude (given atmospheric properties).

Therefore even without a definite geometry for the airplane, one can assess the overall size from the chosen cruise altitude, thus the corresponding length, with some considerations on the general configuration of the aircraft (like length/span ratio, aspect ratio, etc). This point will be later reviewed in more details. Appendices #8 summarizes this idea.

The most critical issue to be addressed is the determination of the aircraft's weight: as underlined earlier, no configuration has been yet specified, and this is not the intent of this study, for which only the *optimized* sonic boom is considered. We want to be able to assess what is the best achievable boom level for given aircraft's parameters, i.e. Mach number, cruise altitude, length, and weight. The absence of a specific configuration makes it both harder and easier to determine the aircraft's weight:

- harder because the different components of the aircraft cannot be sized, thus neither weighted;
- easier since it allows the use of more general concepts for weight calculations, without going into details in geometry analysis of each aircraft's components.

Again, a high level of accuracy for weight calculation is not required, nor can it be achieved anyway, since no configuration has been proposed. Only a broad view of how length and weight will evolve with increasing cruise altitude is needed, in order to assess the resulting optimized sonic boom. At this point of the QSP development process, reliable weight models will provide sufficient estimates of the aircraft's weight, given some aerodynamics and geometry parameters. The weight model that was developed and used for this study is based on Daniel P. Raymer's book.

3.2 WEIGHT BUILD-UP

Calculation of the overpressure of aircraft at different altitudes requires varying the wing loading and hence the size and weight of the aircraft with altitude. This in turn calls for a weight model. The weight model used here is from Daniel P. Raymer's book, *Aircraft Design: A Conceptual Approach*.

Raymer developed different weight models for different types of aircraft, based on historical data. The model chosen was the Fighter/Attack aircraft, considered to be the one matching the largest number of characteristics associated with the QSP. As there was yet no definite design for the supersonic aircraft, some assumptions on aerodynamics properties and design parameters were made. They have been summarized here.

This section is intended to explain what constraints were applied to this model, what parameters were kept constant and what the outputs were.

3.2.1 RAYMER'S MODEL (FIGHTER/ATTACK AIRCRAFT)

Raymer's model gives the weights of the major components in terms of aircraft's parameters (geometric or aerodynamic).

Wing

$$W_{wing} = 0.103 K_{dw} K_{vs} (W_{dg} N_z)^{0.5} S_w^{0.622} A^{0.785} (t/c)_{root}^{-0.4} (1+\lambda)^{0.05} (\cos\Lambda)^{-1} S_{csw}^{0.04}$$

Horizontal tail

$$W_{Horizontaltail} = 3.316 \left(1 + \frac{F_w}{B_h}\right)^{-2} \left(\frac{W_{dg} N_z}{1000}\right)^{0.26} S_{ht}^{0.806}$$

Vertical tail

$$W_{Verticaltail} = 0.452 K_{rht} (1 + H_t / H_v)^{0.5} (W_{dg} N_z)^{0.488} S_{vt}^{0.718} M^{0.341} L_t^{-1} (1 + S_r / S_{vt})^{0.348} A_{vt}^{0.223} (1+\lambda)^{0.25} (\cos\Lambda_{vt})^{-0.323}$$

Fuselage

$$W_{fuselage} = 0.499 K_{dwf} W_{dg}^{0.35} N_z^{0.25} L^{0.5} D^{0.849} W^{0.685}$$

Main Landing Gear

$$W_{mainlandinggear} = K_{cb} K_{tpg} (W_l N_l)^{0.25} L_m^{0.973}$$

Nose Landing Gear

$$W_{noselandinggear} = (W_l N_l)^{0.29} L_n^{0.5} N_{nw}^{0.525}$$

Engine Mounts

$$W_{engmounts} = 0.013 N_{en}^{0.795} T^{0.579} N_z$$

Firewall

$$W_{firewall} = 1.13 S_{fw}$$

Engine section

$$W_{eng\,section} = 0.01 W_{en}^{0.717} N_{en} N_z$$

Air Induction System

$$W_{airinduc} = 13.29 K_{vg} L_d^{0.643} K_d^{0.182} N_{en}^{1.498} (L_s / L_d)^{-0.373} D_e$$

Tailpipe

$$W_{tailpipe} = 3.5 D_e L_{tp} N_{en}$$

Engine Cooling

$$W_{engcooling} = 4.55 D_e L_{sh} N_{en}$$

Oil Cooling

$$W_{oilcooling} = 37.82 N_{en}^{1.023}$$

Engine Controls

$$W_{engcontrols} = 10.5 N_{en}^{1.008} L_{ec}^{0.222}$$

Starter (pneumatic)

$$W_{starter} = 0.025T_e^{0.76} N_{en}^{0.72}$$

Fuel System and Tanks

$$W_{fuelsyst/\tan ks} = 7.45V_t^{0.47}\left(1+\frac{V_i}{V_t}\right)^{-0.095}\left(1+\frac{V_p}{V_t}\right)N_t^{0.066}N_{en}^{0.052}\left(\frac{T.SFC}{1000}\right)^{0.249}$$

Flight Controls

$$W_{flightcont} = 36.28M^{0.003}S_{cs}^{0.489}N_s^{0.484}N_c^{0.127}$$

Instruments

$$W_{instruments} = 8.0 + 36.37N_{en}^{0.676}N_t^{0.237} + 26.4(1+N_{ci})^{1.356}$$

Hydraulics

$$W_{hydraulics} = 37.23K_{vsh}N_u^{0.664}$$

Electrical

$$W_{electricals} = 172.2K_{mc}R_{kva}^{0.152}N_c^{0.10}L_a^{0.10}N_{gen}^{0.091}$$

Avionics

$$W_{avionics} = 2.117W_{uav}^{0.933}$$

Furnishings

$$W_{furnishings} = 217.6N_c$$

Air Conditioning and Anti-ice

$$W_{AC/AI} = 201.6\left[\left(W_{uav} + 200N_c\right)/1000\right]^{0.735}$$

Handling Gear

$$W_{handlinggear} = 3.2\times10^{-4}W_{dg}$$

Parameter definitions:

A	Aspect ratio	-
A_{vt}	Aspect ratio vertical tail	-
B	Span	ft
B_h	Horizontal tail span	ft
D	Fuselage structural depth	ft
D_e	Engine diameter	ft
F_w	Fuselage width at horizontal tail intersection	ft
H_t / H_v	0 for conventional tail, 1 for "T" tail	-
K_{cb}	2.25 for cross-beam gear; 1 otherwise	-
K_d	Duct constant (see Figure 3.5)	-
K_{dw}	0.768 for delta wing; 1 otherwise	-
K_{dwf}	0.774 for delta wing aircraft; 1 otherwise	-
K_{mc}	1.45 if mission completion required after failure	-
K_{rht}	1.047 for rolling tail; 1 otherwise	-
K_{tpg}	0.826 for tripod gear; 1 otherwise	-
K_{vg}	1.62 for variable geometry; 1 otherwise	-
K_{vs}	1.19 fir variable sweep wing; 1 otherwise	-
K_{vsh}	1.425 if variable sweep wing; 1 otherwise	-
λ	Wing sweep at 25% MAC	-
λ_{vt}	Vertical tail sweep	-
L	Fuselage structural length	ft
L_a	Electrical routing distance, generators to avionics to cockpit	ft
L_d	Duct length	ft
L_{ec}	Length from engine front to cockpit	ft
L_m	Length of main landing gear	in
L_n	Nose gear length	in

L_s	Single duct length (see Figure 3.5)	ft
L_{sh}	Length of engine shroud	ft
L_t	Tail length; wing ¼ to tail ¼	ft
L_{tp}	Length of tailpipe	ft
M	Mach number	-
N_c	Number of crew	-
N_{ci}	1 single pilot; 1.2 pilot+backseater; 2.0 pilot+copassenger	-
N_{en}	Number of engines	-
N_{gen}	Number of generators	-
N_l	Ultimate Landing Gear Factor: N_{gear}*1.5	-
N_{nw}	Number of nose wheels	-
N_s	Number of flight control systems	-
N_t	Number of fuel tanks	-
N_u	Number of hydraulic utility functions	-
N_z	Ultimate load factor = 1.5*limit load factor	-
R_{kva}	System electrical rating	-
S_{cs}	Total area of control surfaces	ft^2
S_{csw}	Control surface area (wing mounted)	ft^2
SFC	Specific Fuel Consumption at maximum thrust	-
S_{fw}	Firewall surface area	ft^2
S_{ht}	Horizontal tail area	ft^2
S_r	Rudder area	ft^2
S_{vt}	Vertical tail area	ft^2
S_w	Trapezoidal wing area	ft^2
t/c	Thickness ratio	-
T	Total engine thrust	lb
T_e	Thrust per engine	lb

V_i	Integral tanks volume	gal
V_p	Self-sealing "protected" tanks volume	gal
V_t	Total fuel volume	gal
W	Fuselage structural width	ft
W_{dg}	Design gross weight	lb
W_{en}	Engine weight, each	lb
W_f	Fuel weight	lb
W_l	Landing design gross weight	lb
W_{uav}	Uninstalled avionics weight	lb

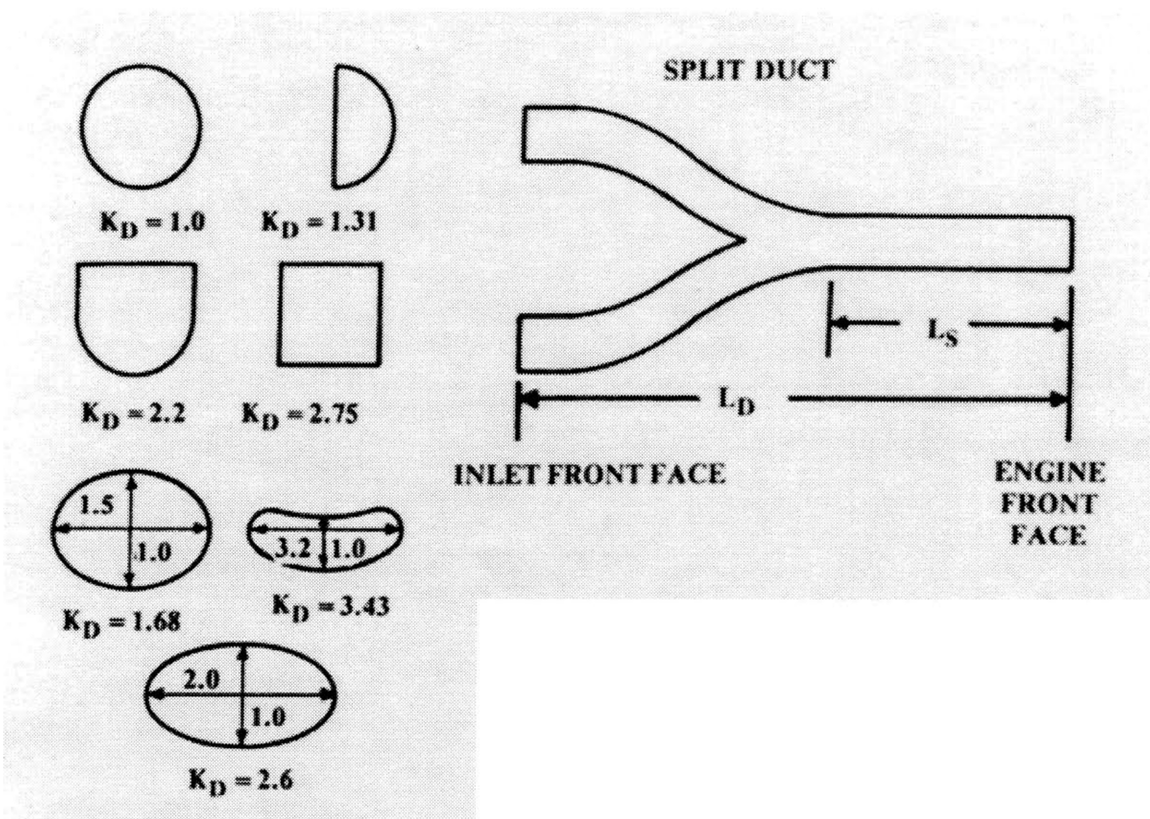

Figure 3.5: Inlet Duct Geometry

3.2.2 ASSUMPTIONS CONSIDERED

No specific configuration had been created for the QSP for the preliminary studies on sonic boom reduction. Therefore, the following design and performance assumptions were established, based both on QSP program goals and on experience.

- Mach number is **2**;
- The lift coefficient C_L is **0.1**;
- The Lift/Drag ratio L/D is **8** (under cruise conditions);
- The range R is 6,000nm (DARPA requirement);
- The specific impulse I is **4220s**; or Specific Fuel Consumption (SFC) at maximum thrust is **1.2**;
- The payload weight $W_{payload}$ is **10,000lbs** (DARPA requirement)
- The wing aspect ratio is **2.67**;
- The ratio between length and span is the same as the Concorde's: L/b = **160/65**;
- The airplane has no horizontal tail;
- The airplane has delta wings;
- There are **2** crew members, a pilot and a back-seater;
- There are **4** engines.

In the altitude/size/weight parametric study, the following parameters were held fixed at their expected values:

A	Aspect ratio	2.67
A_{vt}	Aspect ratio vertical tail	0.8
B_h	Horizontal tail span	0
D	Fuselage structural depth	0.656ft
D_e	Engine diameter	5ft
F_w	Fuselage width at horizontal tail intersection	0
H_t / H_v	0 for conventional tail, 1 for "T" tail	0
K_{cb}	2.25 for cross-beam gear; 1 otherwise	1
K_d	Duct constant	1
K_{dw}	0.768 for delta wing; 1 otherwise	0.768
K_{dwf}	0.774 for delta wing aircraft; 1 otherwise	0.774

K_{mc}	1.45 if mission completion required after failure	1
K_{rht}	1.047 for rolling tail; 1 otherwise	1
K_{tpg}	0.826 for tripod gear; 1 otherwise	1
K_{vg}	1.62 for variable geometry; 1 otherwise	1
K_{vs}	1.19 fir variable sweep wing; 1 otherwise	1
K_{vsh}	1.425 if variable sweep wing; 1 otherwise	1
λ	Wing sweep at 25% MAC	55
λ_{vt}	Vertical tail sweep	65
L_{tp}	Length of tailpipe	2ft
M	Mach number	2
N_c	Number of crew	2
N_{ci}	1 single pilot/1.2 pilot+backseater/2 pilot+copassenger	1.2
N_{en}	Number of engines	4
N_{gen}	Number of generators	4
N_l	Ultimate Landing Gear Factor: N_{gear}*1.5	4.5
N_{nw}	Number of nose wheels	2
N_s	Number of flight control systems	3
N_t	Number of fuel tanks	2
N_u	Number of hydraulic utility functions	2
N_z	Ultimate load factor = 1.5*limit load factor	6
R_{kva}	System electrical rating	5
SFC	Specific Fuel Consumption at maximum thrust	1.2
S_{fw}	Firewall surface area	80ft^2
S_{ht}	Horizontal tail area	0
t/c	Thickness ratio	0.03
W	Fuselage structural width	10ft
W_{uav}	Uninstalled avionics weight	1000lb

We also assumed that since this model was for a Fighter/Attack aircraft, the cabin pressure weight, in the case of the QSP, needed to be added to the overall calculated weight. We assigned 2000lbs for cabin pressure weight.

3.2.3 INFLUENCE OF ALTITUDE

The following parameters were assumed to depend on the altitude Z:

- Speed: $V(Z) = Ma(Z) = 2\sqrt{\gamma RT(Z)}$
- Wing loading: $\frac{W}{S_w}(Z) = \frac{1}{2}\frac{\rho(Z)C_L V(Z)^2}{g}$
- Fuel weight fraction: Breguet equation gives the range R as $R = V(Z)I\frac{L}{D}\ln\left(\frac{W_0 - W_f(Z)}{W_0}\right)$ where W_0 is the gross take-off weight, and W_f the fuel weight: thus the fuel weight fraction is $\frac{W_f}{W_0}(Z) = 1 - e^{-\frac{R}{V(Z)I L/D}}$
- Thrust/Weight ratio: $\frac{T}{W_{eng}}(Z) = 1.55e^{\frac{60000-Z}{22240}}$, where Z is in ft.

3.2.4 LINKS BETWEEN PARAMETERS

The following parameters were assumed to depend directly on other parameters:

B	Span	
L	Fuselage structural length	$B \times \frac{160}{65}$
L_a	Electrical routing distance	$0.6L$
L_d	Duct length	$0.3L$
L_{ec}	Length from engine front to cockpit	$0.4L$
L_m	Length of main landing gear	$12 \times 0.06L$
L_n	Nose gear length	$12 \times 0.08L$
L_s	Single duct length	$0.5L_d$
L_{sh}	Length of engine shroud	$0.06L$
L_t	Tail length; wing ¼ to tail ¼	$0.5L$
S_{cs}	Total area of control surfaces	$0.1S_w$

S_{csw}	Control surface area (wing mounted)	$0.1S_w$
S_r	Rudder area	$0.05S_w$
S_{vt}	Vertical tail area	$0.1S_w$
S_w	Trapezoidal wing area	$\frac{B^2}{A}$
T	Total engine thrust	$\frac{W_0}{8}$
T_e	Thrust per engine	$\frac{W_0}{32}$
V_i	Integral tanks volume	$1.2V_t$
V_p	Self-sealing "protected" tanks volume	$0.6V_t$
V_t	Total fuel volume	$\frac{W_f}{7.09}$
W_{dg}	Design gross weight	W_0
W_{en}	Engine weight, each	$\frac{1}{4}\frac{T}{\left(T/W_{eng}\right)(Z)}$
W_f	Fuel weight	$W_0\left(\frac{W_f}{W_0}\right)(Z)$
W_l	Landing design gross weight	$W_0 - W_f$

Once an altitude is specified, all these parameters are determined, using the assumptions given earlier. However, some of the inputs to the weight model are also outputs (among them, design gross weight and span). We therefore need to consider an iterative process.

3.2.5 Weight Calculation Iteration

We previously stated what parameters were directly determined by cruise altitude, taking into account the assumptions on performance and design parameters. Among them was the wing loading: $\frac{W}{S_w}(Z) = \frac{1}{2}\frac{\rho(Z)C_L V(Z)^2}{g}$. Thus, once cruise altitude has been set, if we first assume a certain take-off gross weight (TOGW) W_0, we have access to the required wing area S_w. As aspect ratio A has been fixed, this will give the required span $B = \sqrt{AS_w}$. Looking back at the parameters that are linked to each other, we verify that they can all be determined from that, including length (since length/span ratio has been fixed). At the end, we therefore get a value for the resulting take-off gross weight W_{dg}, which is the final output of the weight model.

The following diagram (Figure 3.6) summarizes this iteration:

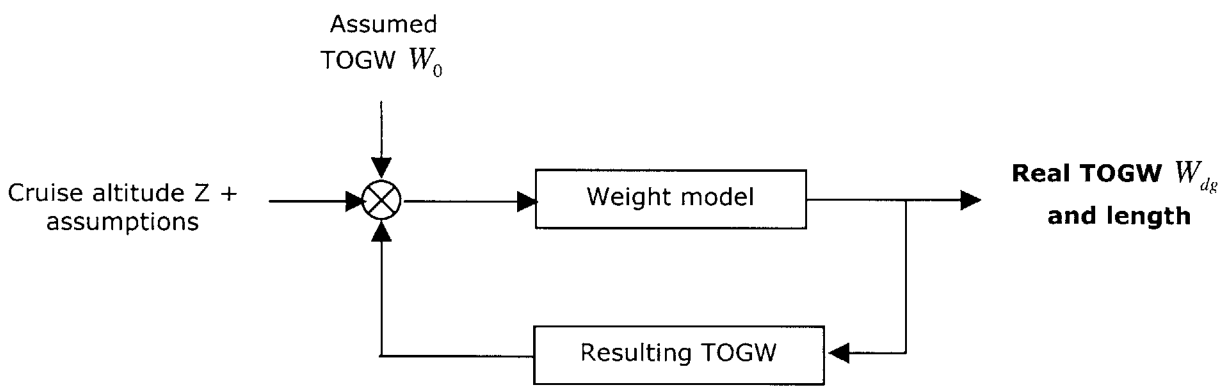

Figure 3.6: Weight calculation process

Thus, for each given cruise altitude, we start the model with an assumed W_0, usually 100,000lbs, then introduce it into the weight model. The resulting weight W_{dg} is then either higher or lower than 100,000lbs: if it is higher, then a higher input value of W_0 is used in the next iteration. If it is lower, a lower value of W_0 is used.

The iteration process eventually leads to a value such that input weight and output weight are the same.

3.2.6 Results for different altitudes

For each altitude, take-off gross weight was assessed, using the iteration process previously described. Required wing area, corresponding span and length are additional outputs of the weight model.

Therefore, for each altitude, we were able to determine:

- the required wing area;
- the corresponding span of the aircraft;
- the length of the aircraft;
- its take-off gross weight.

We looked at cruising altitudes ranging from 30,000ft to 70,000ft. Results have been summarized in Figures 3.7 and 3.8.

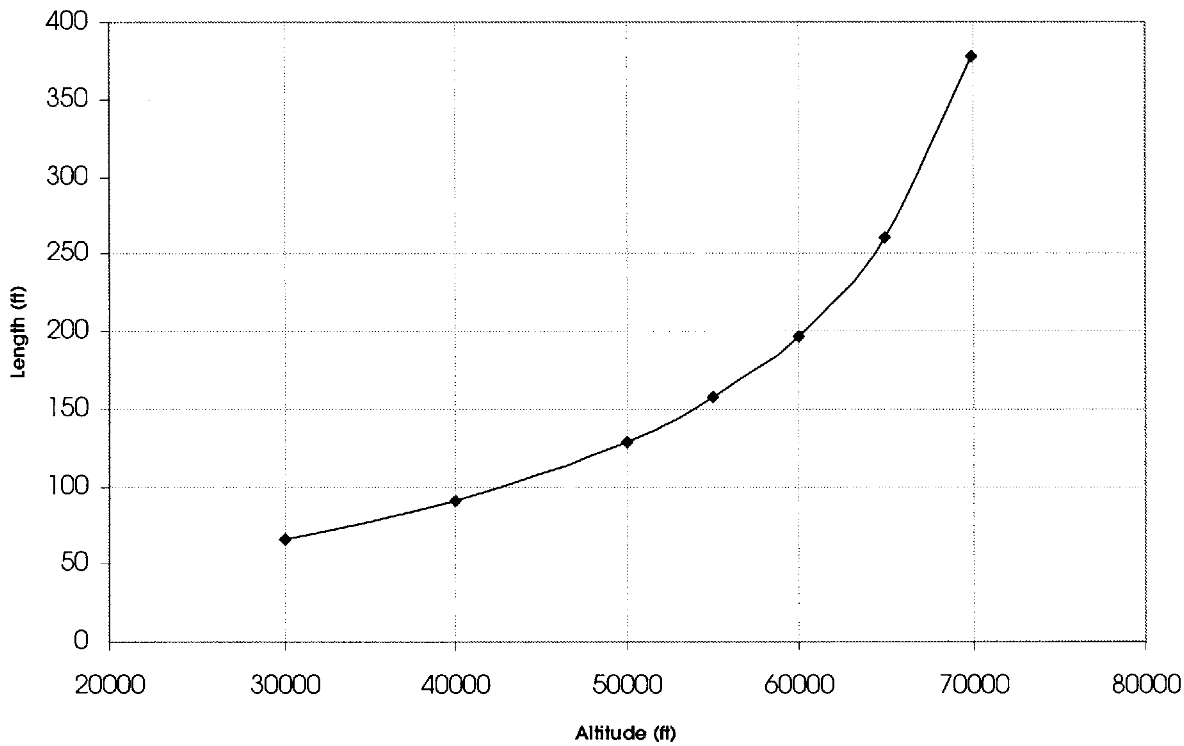

Figure 3.7: Required aircraft length vs. cruise altitude

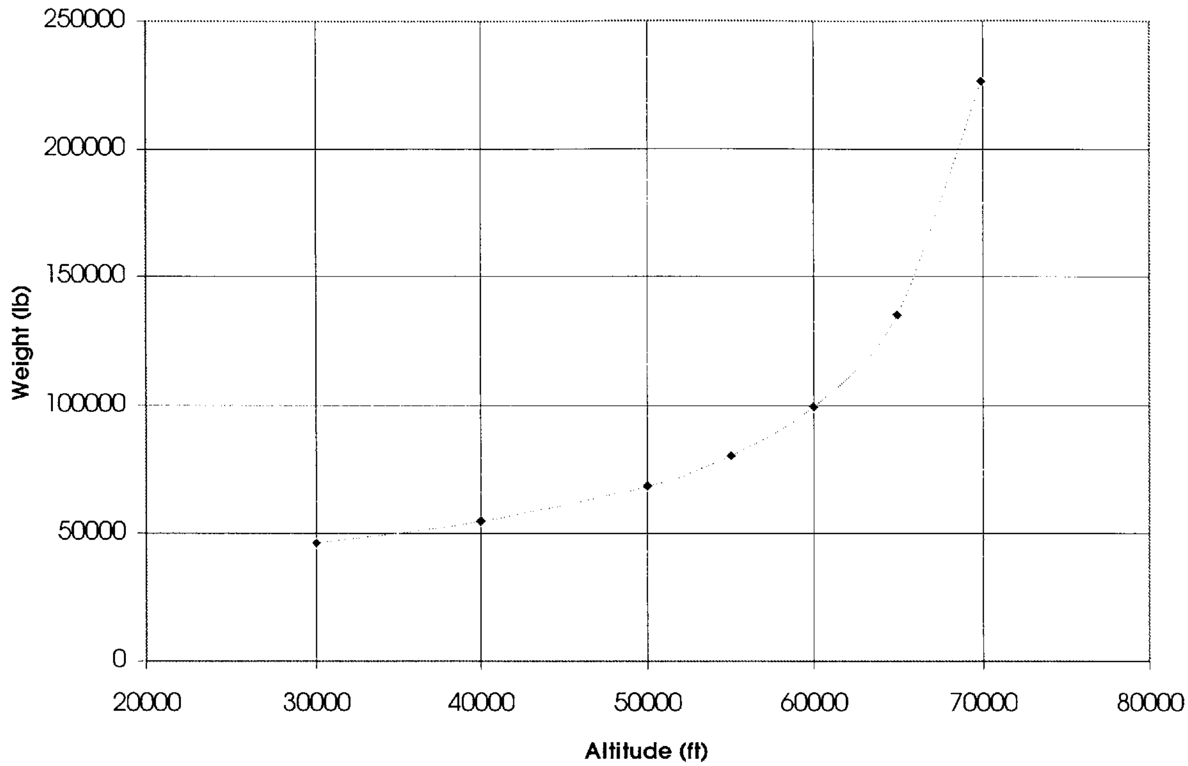

Figure 3.8: Required aircraft weight vs. cruise altitude

(Detailed results for each cruise altitude (including individual weights of aircraft's components) can be found in appendices (Excel tables).)

3.3 Conclusion

As outlined earlier, role of altitude in sonic boom minimization was not clear, since we only looked at variation of boom levels vs. altitude with *constant length and weight*. Now we have determined how the aircraft should be sized (wing area, span and length) and what its resulting weight would be, when changing the assigned cruise altitude.

Therefore, we can now look at how cruise altitude *actually* affects sonic boom level (again, we are talking here about *optimized* boom level, each cruising altitude corresponding to a different aircraft, for which the sonic boom is the *best achievable* one for this particular aircraft). To do this, we use the results obtained in the previous table to input specific (and realistic) sets of flight parameters (Mach number, cruise altitude, length, and weight) in the Seeb code.

Figure 3.9 and Figure 3.10 summarize the results obtained:

Altitude	Wing loading (lb/sqft)	**Span (ft)**	Length (ft)	Wing area (sqft)	**Total Weight (lb)**	**Overpressure (psf)**
30000	172,5072108	**26,73579**	65,81118343	267,7163452	**46183,65558**	**0,5046**
40000	107,6819636	**36,84615**	90,69820652	508,4788406	**54754,34247**	**0,4032**
50000	66,72138013	**52,32183**	128,7921939	1025,308527	**68410,79513**	**0,3460**
55000	52,43834767	**63,88265**	157,2495896	1528,461585	**80150,73281**	**0,3276**
60000	41,36395537	**79,87502**	196,6154287	2389,520033	**98840,16699**	**0,3165**
65000	32,34309276	**105,5679**	259,859362	4173,997861	**135000,396**	**0,3136**
70000	25,65078615	**153,6141**	378,1269893	8837,935752	**226703,2213**	**0,3336**

Figure 3.9: Table for realistic sets of flight parameters, and corresponding optimized boom level

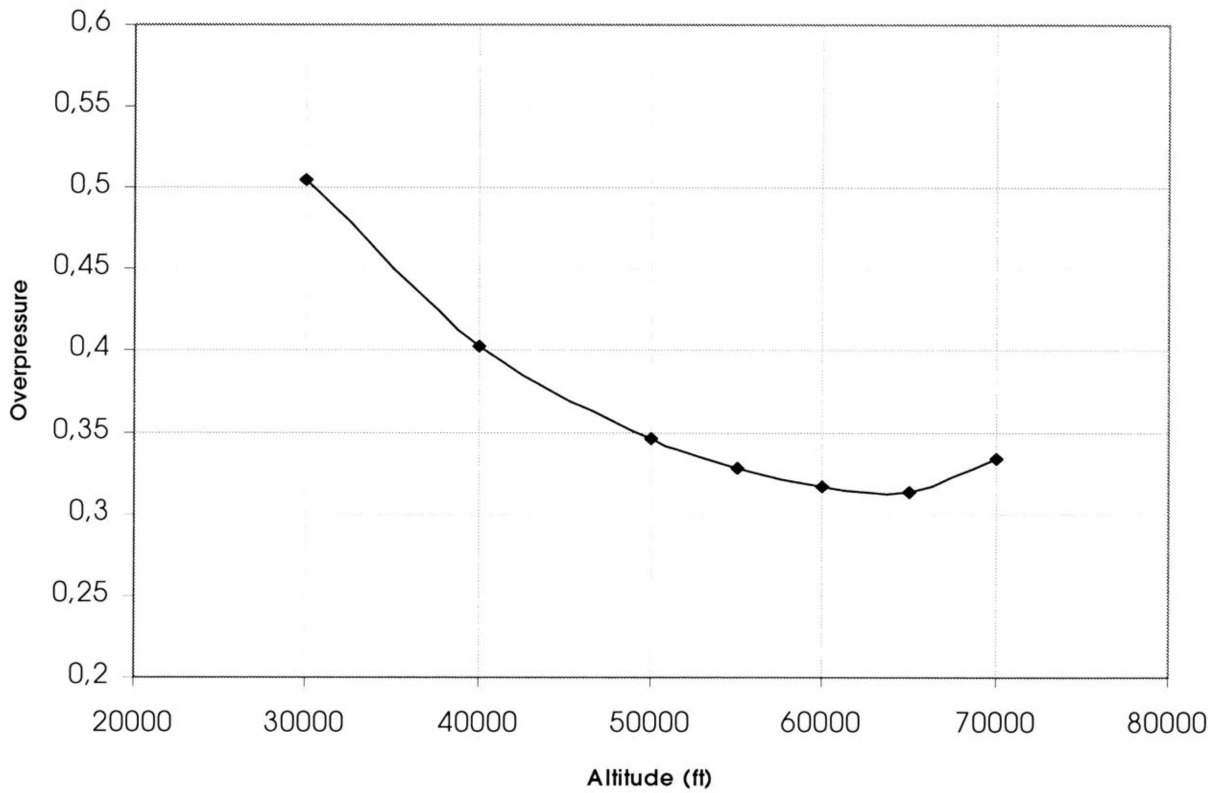

Figure 3.10: Optimized sonic boom level vs. cruise altitude

It is now clear that the answer to sonic boom minimization is not necessarily flying higher. What happens when cruise altitude is increased is that the aircraft (again, a different one for each chosen cruise altitude) gets bigger, thus both longer and heavier. At first, the influence of length on the resulting sonic boom overpasses the influence of weight: the aircraft gets longer "faster" than it gets heavier. But after a certain altitude has been passed (the *best* cruise altitude, for which the optimized sonic boom is the lowest), the aircraft gets so big that weight dominates the length.

What this graph also shows is that there exists an *optimum* cruise altitude. For this altitude, the corresponding aircraft is such that if we optimize its shape (following the Seeb code's recommendations to reduce the sonic boom), the resulting boom level it will produce on the ground is the best achievable one, all cruise altitudes considered.

As highlighted in the table of Figure 3.9, this optimized cruise altitude is **60,000ft**. It should be considered as the one leading to the highest potential reduction in boom level on the ground.

The corresponding length, span, weight, wing area and optimized sonic boom level for this chosen cruise altitude are the following, taken from the table of Figure 3.9:

- Length: **196.6ft**
- Span: **79.9ft**
- Weight: **98,840lb**
- Wing area: **2389.5sqft**
- Optimized sonic boom: **0.3165psf**

The Seeb code gives the recommended equivalent area distribution for those parameters, in order to reach the optimized value of 0.3165psf for the boom level: given those design and flight parameters (length, span, wing area, weight, and previously stated Mach number, aspect ratio, etc), the shape of the aircraft should be such that its equivalent area distribution should match the one represented on Figure 3.11, in order to achieve the minimum sonic boom level:

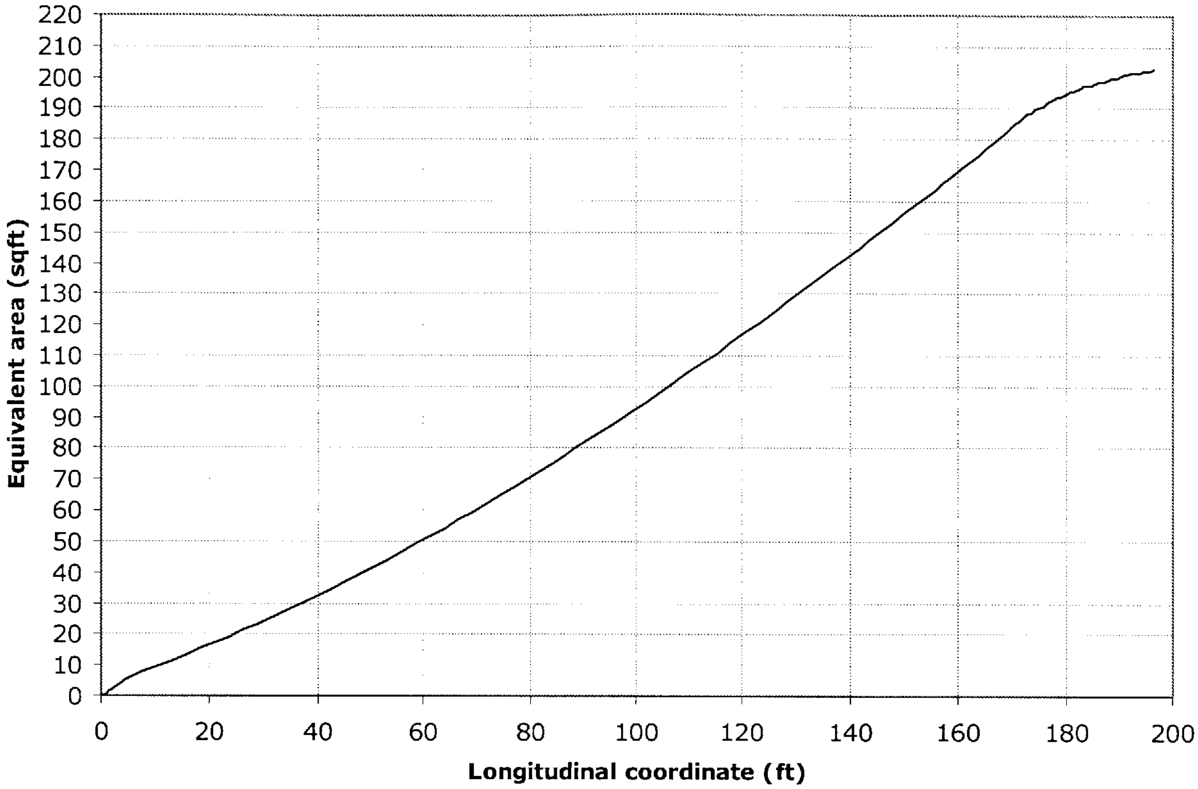

Figure 3.11: Recommended Equivalent Area Distribution

4 PROPOSAL OF A POSSIBLE CONFIGURATION FOR THE QSP

After we have assessed what the flight and design parameters for the aircraft should be, in order to achieve the minimum sonic boom and meet DARPA requirements, we can look at a first draft for a possible configuration.

This configuration has been determined from the proposed set of parameters (length, span, wing area and weight). There was no specific rule that lead to this drawing: it is mainly based on experience, and should only be considered as a first sketch of what the aircraft *could* look like.

The proposed configuration can be found in the appendices.

5 CONCLUSION

This study was based on today's new challenges for the future of supersonic flight: allowing for overland flight, in order to meet economics and performance criteria. DARPA imposed a maximum value of 0.3psf for the overpressure level on the ground for an aircraft flying at cruise conditions.

Thanks to review of relevant documents, we were able to assemble elements of history in sonic boom reduction. Then attention was focused on understanding the boom phenomenon: how it is created, how it propagates, and how it can eventually be reduced. Finally, the theory underlying the reduction of sonic boom was reviewed, including how to access to design requirements.

The influence of flight and design parameters was determined by using the Seeb code developed by Christine Darden. Using this program, we were able to assess how Mach number, length, weight and cruise altitude, respectively, affected the *optimized* sonic boom level, i.e. the best achievable overpressure level, once configuration has been optimized in order to meet the equivalent area distribution required to minimize the boom.

Following those findings, a weight model was used in order to only consider realistic sets of parameters, as cruise altitude affected the required size (length and weight) of the aircraft. Assumptions based on requirements or experience were formulated. Then, for each altitude, the required length, span, wing area and weight of the aircraft were determined, using an iterative process to reach the take-off gross weight of the aircraft. Finally, corresponding sets of parameters for each cruise altitude were input into the Seeb code, in order to assess the best achievable sonic boom level for each of them, and give some elements of decision in terms of cruise altitude.

The results showed the existence of an optimized cruise altitude. For this particular altitude, design parameters were assessed, as well as the corresponding equivalent area distribution required to meet boom minimization criteria. Finally, a possible configuration for the QSP was presented.

The 0.3psf goal has been demonstrated to be achievable. It corresponds to the best achievable sonic boom level for a given set of aircraft requirements. To realize this optimum solution, the equivalent area distribution of the actual aircraft (whose length, span and weight should be as close as possible to those determined for this cruise altitude) should match the one given by the Seeb code that will eventually lead to boom minimization. As there are an infinite number of designs for the same equivalent area distribution, there remains the task to link a modification in this distribution to a change in the aircraft's actual configuration.

This is where the challenge for sonic boom minimization lies: there is no unique configuration for which the overpressure on the ground would be minimized. What this study reviewed is how design and flight parameters can affect the best level one can hope to reach by using minimization principles. It lead to the unique finding of how cruise altitude *realistically* affects boom "performance", and to the existence of an optimizing cruise altitude, given certain assumptions.

Caution should be taken regarding the way weight was estimated. The model used was based on historical data, and was applied to an aircraft for which no specific detailed configuration had been yet defined. One can expect that modern methods of weight reduction can lead to smaller weights for an aircraft with the same size (length, span and wing area). This will of course imply lower levels of sonic boom.

Finally, the configuration presented here was just a "best" estimate of what the aircraft should look like, but it can be (and should be) used as a starting point for possible configurations. Design analysis codes for sonic boom calculation are available to extract the equivalent area distribution, and hence the F-function, and the sonic boom level of an aircraft with a specific configuration.

Therefore, a possible process for sonic boom reduction is as follows:

1. Start from a "best-guessed" configuration, based on experience, performance requirements, and considerations of length (the longer the aircraft, the smaller the sonic boom) and weight (the lighter, the better);
2. Calculate the approximated weight of this aircraft, and input flight and design parameters into the Seeb code;

3. Use the resulting recommended equivalent area distribution to modify the existing configuration in order to match this distribution;
4. Readjust weight and length in boom calculation.

Other approaches could conceivably be used, depending on the planned work and on available methods and resources. Sonic boom reduction is not an easy and catalogued process known by every single aerodynamics engineer. Instead, it requires experience in numerous fields, and exploration of still unknown areas.

References

1. Darden, Christine M.: *The Importance of Sonic Boom Research in the Development of Future High Speed Aircraft*. JOURNAL of the NTA/Winter 1992.

2. Thomas, Charles L.: *Extrapolation of Sonic Boom Pressure Signatures by the Waveform Parameter Method*. NASA TN D-6832, 1972.

3. Hayes, Wallace D.; Haefeli, Rudolph C.; and Kulsrud, H. E.: *Sonic Boom Propagation in a Stratified Atmosphere, with Computer Program*. NASA CR-1299, 1969.

4. Harris, Roy V., Jr.: *An Analysis and Correlation of Aircraft Wave Drag*. NASA TM X-947, 1964.

5. Cliff, Susan E.; and Thomas, Scott D.: *Euler/Experiment Correlations of Sonic Boom Pressure Signatures*. AIAA Paper 91-32/6, 1991.

6. Carlson, Harry W.; Barger, Raymond L.; and Mack, Robert J.: *Application of Sonic-Boom Minimization Concept in Supersonic Transport Design*. NASA TN D-7218, 1973.

7. Carlson, Harry W.; McLean, F. Edward; and Shrout, Barrett L.: *A Wind-Tunnel Study of Sonic-Boom Characteristics for Basic and Modified Models of a Supersonic Transport Configuration*. NASA TM X-1236, 1966.

8. Durston, Don: *NFBOOM Code*. NASA Ames, AAL, 1997

9. Needleman, K; and Mack, R: *A Study of Sonic Boom Overpressure Trends with Respect to Weight, Altitude, Mach Number and Vehicle Shaping*. AIAA 90-0367, 1990.

10. Darden, Christine M.: *Sonic-Boom Minimization with Nose-Bluntness Relaxation*. NASA TP-1348, 1979.

11. Mack, Robert J.; and Needleman, Kathy E.: *A Semiempirical Method for Obtaining Fuselage Normal Areas From Fuselage Mach Sliced Areas*. NASA TM-4228, 1990.

12. Barger, Raymond L.; and Adams, Mary S.: *Fuselage Design for a Specified Mach-Sliced Area Distribution*. NASA TP-2975, 1990.

13. Barger, Raymond L.: *Design of Bodiest to Produce Specified Sonic-Boom Signatures.* NASA TN D-4704, 1968.

14. Mack, Robert J.: *Nacelle Integration to Reduce the Sonic Boom of Aircraft Designed to Cruise at Supersonic Speeds.* NASA TM-1999-209534, 1999.

15. Rech, Jean; and Leyman, Clive S.: *A Case Study by Aerospatiale and British Aerospace on the Concorde*. AIAA Professional Studies.

16. Woodward, Frank A.: *Analysis and Design of Wing-Body Combinations at Subsonic and Supersonic Speeds*. Journal of Aircraft, Vol. 5, NO. 6, 1968.

6 APPENDICES

Appendices #1: Weight model results for cruise altitude Z=30,000ft

Span	***Bh***	***ft***	***26,7358***
Aspect ratio	***A***		***2,67***
Aspect ratio vertical tail	Avt		0,8
Horizontal tail span	Bh	ft	0
Fuselage structural depth	D	ft	0,656
Engine diameter	De	ft	5
Fuselage width at horizontal tail intersection	Fw	ft	0
0 for conventional tail, 1 for "T" tail	Ht/Hv		0
2.25 for cross-beam gear; 1 otherwise	Kcb		1
Duct constant (see Fig)	Kd		1
0.768 for delta wing; 1 otherwise	Kdw		0,768
0.774 for delta wing aircraft; 1 otherwise	Kdwf		0,774
1.45 if mission completion required after failure	Kmc		1
1.047 for rolling tail; 1 otherwise	Krht		1
0.826 for tripod gear; 1 otherwise	Ktpg		1
1.62 for variable geometry; 1 otherwise	Kvg		1
1.19 for variable sweep wing; 1 otherwise	Kvs		1
1.425 if variable sweep wing; 1 otherwise	Kvsh		1
Wing sweep at 25% MAC	LAMBDA		55
Vertical tail sweep	LAMBDAvt		65
Fuselage structural length	**L**	ft	**65,81118**
Electrical routing distance, generators to avionics to cockpit	**La**	ft	39,48671
Duct length	**Ld**	ft	19,74336
Length from engine front to cockpit	**Lec**	ft	26,32447
Length of main landing gear	**Lm**	in	47,38405
Nose gear length	**Ln**	in	63,17874
Single duct length (see Fig)	**Ls**	??	9,871678
Length of engine shroud	**Lsh**	ft	3,948671
Tail length; wing 1/4 to tail 1/4	Lt	ft	32,90559
Length of tailpipe	Ltp	ft	2
Mach number	M		2
Number of crew	Nc		2
1 single pilot; 1.2 pilot+backseater; 2.0 pilot+copassenger	Nci		1,2
Number of engines	Nen		4
Number of generators	Ngen		4
Ultimate Landing Load Factor: Ngear*1.5	Nl		4,5
Number of nose wheels	Nnw		2
Number of flight control systems	Ns		3
Number of fuel tanks	Nt		2
Number of hydraulic utility functions	Nu		2
Ultimate load factor = 1.5*limit load factor	Nz		6
System electrical rating	Rkva		5
Total area of control surfaces	**Scs**	ft2	26,77163
Control surface area (wing mounted)	**Scsw**	ft2	26,77163
Specific Fuel Consumption at maximum thrust	SFC		1,2
Firewall surface area	Sfw	ft2	80
Horizontal tail area	Sht	ft2	0
Rudder area	**Sr**	ft2	13,38582
Vertical tail area	**Svt**	ft2	26,77163
Trapezoidal Wing Area	**Sw**	ft2	**267,7163**
Thickness ratio	t/c		0,03
Total engine thrust	**T**	lb	**5772,875**
Thrust per engine	**Te**	lb	1443,219
Integral tanks volume	**Vi**	gal	3271,14
Self-sealing "protected" tanks volume	**Vp**	gal	1635,57
Total fuel volume	**Vt**	gal	2725,95
Fuselage structural width	W	ft	10
Design gross weight	**Wdg**	lb	46183
Engine weight, each	**Wen**	lb	**241,6415**
Fuel weight	**Wf**	lb	19326,99
Landing design gross weight	**Wl**	lb	26856,01
Uninstalled avionics weight	Wuav	lb	1000

Wing	2371,604932		
Horizontal Tail	0		
Vertical Tail	125,1000895		
Fuselage	712,2775858		
Cabin pressure	2000		
Main Landing Gear	796,0743802		
Nose Landing Gear	340,5492259		
Engine Mounts	35,36538195		
Firewall	90,4		
Engine Section	12,27284537		
Air Induction System	4673,268295		
Tailpipe	140		
Engine Cooling	359,3290615		
Oil Cooling	156,1812504		
Engine Controls	87,77798799		
Starter	17,08109255		
Fuel System and Tanks	829,6929139		
Flight Controls	337,1792848		
Instruments	194,3162664		
Hydraulics	58,98980402		
Electrical	386,1998863		
Avionics	1332,664589		
Furnishings	543,2		
Air Conditioning and Anti-Ice	258,1633774		
Handling Gear	14,77856		
Lavatories	17,63732272		
			W/Wtotal
Wempty	**15890,10413**		0,344063
Wgross first estimate	**46183**		
Swing	267,7163452	ft2	
Wfuel	**19326,98533**		0,418481
Wpayload	10000		0,216527
Wengines	**966,56612**		0,020929
Wtotal	**46183,66**		1
Swing	267,7201455	ft2	
Altitude	***30000***	ft	
W/S(Z)	***172,50721***	lb/ft2	
Speed(Z)	***607,01603***	m/s	
T/Weng(Z)	***5,9725609***		
Wf/W0(Z)	***0,418487***		

Appendices #2: Weight model results for cruise altitude Z=40,000ft

Span	***Bh***	***ft***	***36,8461***
Aspect ratio	***A***		***2,67***
Aspect ratio vertical tail	Avt		0,8
Horizontal tail span	Bh	ft	0
Fuselage structural depth	D	ft	0,656
Engine diameter	De	ft	5
Fuselage width at horizontal tail intersection	Fw	ft	0
0 for conventional tail, 1 for "T" tail	Ht/Hv		0
2.25 for cross-beam gear; 1 otherwise	Kcb		1
Duct constant (see Fig)	Kd		1
0.768 for delta wing; 1 otherwise	Kdw		0,768
0.774 for delta wing aircraft; 1 otherwise	Kdwf		0,774
1.45 if mission completion required after failure	Kmc		1
1.047 for rolling tail; 1 otherwise	Krht		1
0.826 for tripod gear; 1 otherwise	Ktpg		1
1.62 for variable geometry; 1 otherwise	Kvg		1
1.19 for variable sweep wing; 1 otherwise	Kvs		1
1.425 if variable sweep wing; 1 otherwise	Kvsh		1
Wing sweep at 25% MAC	LAMBDA		55
Vertical tail sweep	LAMBDAvt		65
Fuselage structural length	**L**	ft	**90,69821**
Electrical routing distance, generators to avionics to cockpit	**La**	ft	54,41892
Duct length	**Ld**	ft	27,20946
Length from engine front to cockpit	**Lec**	ft	36,27928
Length of main landing gear	**Lm**	in	65,30271
Nose gear length	**Ln**	in	87,07028
Single duct length (see Fig)	**Ls**	??	13,60473
Length of engine shroud	**Lsh**	ft	5,441892
Tail length; wing 1/4 to tail 1/4	Lt	ft	45,3491
Length of tailpipe	Ltp	ft	2
Mach number	M		2
Number of crew	Nc		2
1 single pilot; 1.2 pilot+backseater; 2.0 pilot+copassenger	Nci		1,2
Number of engines	Nen		4
Number of generators	Ngen		4
Ultimate Landing Load Factor: Ngear*1.5	Nl		4,5
Number of nose wheels	Nnw		2
Number of flight control systems	Ns		3
Number of fuel tanks	Nt		2
Number of hydraulic utility functions	Nu		2
Ultimate load factor = 1.5*limit load factor	Nz		6
System electrical rating	Rkva		5
Total area of control surfaces	**Scs**	ft2	50,84788
Control surface area (wing mounted)	**Scsw**	ft2	50,84788
Specific Fuel Consumption at maximum thrust	SFC		1,2
Firewall surface area	Sfw	ft2	80
Horizontal tail area	Sht	ft2	0
Rudder area	**Sr**	ft2	25,42394
Vertical tail area	**Svt**	ft2	50,84788
Trapezoidal Wing Area	**Sw**	ft2	**508,4788**
Thickness ratio	t/c		0,03
Total engine thrust	**T**	lb	**6844,25**
Thrust per engine	**Te**	lb	1711,063
Integral tanks volume	**Vi**	gal	3958,749
Self-sealing "protected" tanks volume	**Vp**	gal	1979,375
Total fuel volume	**Vt**	gal	3298,958
Fuselage structural width	W	ft	10
Design gross weight	**Wdg**	lb	54754
Engine weight, each	**Wen**	lb	**449,1398**
Fuel weight	**Wf**	lb	23389,61
Landing design gross weight	**Wl**	lb	31364,39
Uninstalled avionics weight	Wuav	lb	1000

Wing	3948,581212		
Horizontal Tail	0		
Vertical Tail	156,3405497		
Fuselage	887,5147434		
Cabin pressure	2000		
Main Landing Gear	1130,681764		
Nose Landing Gear	418,1903642		
Engine Mounts	39,02886947		
Firewall	90,4		
Engine Section	19,14118572		
Air Induction System	5743,676499		
Tailpipe	140		
Engine Cooling	495,2122076		
Oil Cooling	156,1812504		
Engine Controls	94,25621579		
Starter	19,44040311		
Fuel System and Tanks	946,8268271		
Flight Controls	461,4188219		
Instruments	194,3162664		
Hydraulics	58,98980402		
Electrical	398,7879634		
Avionics	1332,664589		
Furnishings	543,2		
Air Conditioning and Anti-Ice	258,1633774		
Handling Gear	17,52128		
Lavatories	17,63732272		
			W/Wtotal
Wempty	**19568,17152**	0,357381	
Wgross first estimate	**54754**		
Swing	508,4788406 ft2		
Wfuel	**23389,61158**	0,427174	
Wpayload	10000	0,182634	
Wengines	**1796,559375**	0,032811	
Wtotal	**54754,34**	1	
Swing	508,482021 ft2		
Altitude	***40000*** ft		
W/S(Z)	***107,68196*** lb/ft2		
Speed(Z)	***590,614*** m/s		
T/Weng(Z)	***3,8096431***		
Wf/W0(Z)	***0,4271763***		

Appendices #3: Weight model results for cruise altitude Z=50,000ft

Span	***Bh***	***ft***	***52,3218***
Aspect ratio	***A***		***2,67***
Aspect ratio vertical tail	Avt		0,8
Horizontal tail span	Bh	ft	0
Fuselage structural depth	D	ft	0,656
Engine diameter	De	ft	5
Fuselage width at horizontal tail intersection	Fw	ft	0
0 for conventional tail, 1 for "T" tail	Ht/Hv		0
2.25 for cross-beam gear; 1 otherwise	Kcb		1
Duct constant (see Fig)	Kd		1
0.768 for delta wing; 1 otherwise	Kdw		0,768
0.774 for delta wing aircraft; 1 otherwise	Kdwf		0,774
1.45 if mission completion required after failure	Kmc		1
1.047 for rolling tail; 1 otherwise	Krht		1
0.826 for tripod gear; 1 otherwise	Ktpg		1
1.62 for variable geometry; 1 otherwise	Kvg		1
1.19 for variable sweep wing; 1 otherwise	Kvs		1
1.425 if variable sweep wing; 1 otherwise	Kvsh		1
Wing sweep at 25% MAC	LAMBDA		55
Vertical tail sweep	LAMBDAvt		65
Fuselage structural length	**L**	ft	**128,7922**
Electrical routing distance, generators to avionics to cockpit	**La**	ft	77,27532
Duct length	**Ld**	ft	38,63766
Length from engine front to cockpit	**Lec**	ft	51,51688
Length of main landing gear	**Lm**	in	92,73038
Nose gear length	**Ln**	in	123,6405
Single duct length (see Fig)	**Ls**	??	19,31883
Length of engine shroud	**Lsh**	ft	7,727532
Tail length; wing 1/4 to tail 1/4	Lt	ft	64,3961
Length of tailpipe	Ltp	ft	2
Mach number	M		2
Number of crew	Nc		2
1 single pilot; 1.2 pilot+backseater; 2.0 pilot+copassenger	Nci		1,2
Number of engines	Nen		4
Number of generators	Ngen		4
Ultimate Landing Load Factor: Ngear*1.5	Nl		4,5
Number of nose wheels	Nnw		2
Number of flight control systems	Ns		3
Number of fuel tanks	Nt		2
Number of hydraulic utility functions	Nu		2
Ultimate load factor = 1.5*limit load factor	Nz		6
System electrical rating	Rkva		5
Total area of control surfaces	**Scs**	ft2	102,5309
Control surface area (wing mounted)	**Scsw**	ft2	102,5309
Specific Fuel Consumption at maximum thrust	SFC		1,2
Firewall surface area	Sfw	ft2	80
Horizontal tail area	Sht	ft2	0
Rudder area	**Sr**	ft2	51,26543
Vertical tail area	**Svt**	ft2	102,5309
Trapezoidal Wing Area	**Sw**	ft2	**1025,309**
Thickness ratio	t/c		0,03
Total engine thrust	**T**	lb	**8551,25**
Thrust per engine	**Te**	lb	2137,813
Integral tanks volume	**Vi**	gal	4946,087
Self-sealing "protected" tanks volume	**Vp**	gal	2473,044
Total fuel volume	**Vt**	gal	4121,739
Fuselage structural width	W	ft	10
Design gross weight	**Wdg**	lb	68410
Engine weight, each	**Wen**	lb	**879,7547**
Fuel weight	**Wf**	lb	29223,13
Landing design gross weight	**Wl**	lb	39186,87
Uninstalled avionics weight	Wuav	lb	1000

Wing	7021,437251		
Horizontal Tail	0		
Vertical Tail	203,0775271		
Fuselage	1143,318697		
Cabin pressure	2000		
Main Landing Gear	1681,493961		
Nose Landing Gear	531,5737505		
Engine Mounts	44,39943424		
Firewall	90,4		
Engine Section	30,99691853		
Air Induction System	7196,361684		
Tailpipe	140		
Engine Cooling	703,2053789		
Oil Cooling	156,1812504		
Engine Controls	101,8869511		
Starter	23,02502485		
Fuel System and Tanks	1111,221263		
Flight Controls	650,1832088		
Instruments	194,3162664		
Hydraulics	58,98980402		
Electrical	413,0200412		
Avionics	1332,664589		
Furnishings	543,2		
Air Conditioning and Anti-Ice	258,1633774		
Handling Gear	21,8912		
Lavatories	17,63732272		
			W/Wtotal
Wempty	**25668,6449**	0,375213	
Wgross first estimate	**68410**		
Swing	1025,308527 ft2		
Wfuel	**29223,13125**	0,427171	
Wpayload	10000	0,146176	
Wengines	**3519,018982**	0,05144	
Wtotal	**68410,8**	1	
Swing	1025,320444 ft2		
Altitude	***50000*** ft		
W/S(Z)	***66,72138*** lb/ft2		
Speed(Z)	***590,614*** m/s		
T/Weng(Z)	***2,4300096***		
Wf/W0(Z)	***0,4271763***		

Appendices #4: Weight model results for cruise altitude Z=55,000ft

Span	***Bh***	***ft***	***63,8826***
Aspect ratio	***A***		***2,67***
Aspect ratio vertical tail	Avt		0,8
Horizontal tail span	Bh	ft	0
Fuselage structural depth	D	ft	0,656
Engine diameter	De	ft	5
Fuselage width at horizontal tail intersection	Fw	ft	0
0 for conventional tail, 1 for "T" tail	Ht/Hv		0
2.25 for cross-beam gear; 1 otherwise	Kcb		1
Duct constant (see Fig)	Kd		1
0.768 for delta wing; 1 otherwise	Kdw		0,768
0.774 for delta wing aircraft; 1 otherwise	Kdwf		0,774
1.45 if mission completion required after failure	Kmc		1
1.047 for rolling tail; 1 otherwise	Krht		1
0.826 for tripod gear; 1 otherwise	Ktpg		1
1.62 for variable geometry; 1 otherwise	Kvg		1
1.19 for variable sweep wing; 1 otherwise	Kvs		1
1.425 if variable sweep wing; 1 otherwise	Kvsh		1
Wing sweep at 25% MAC	LAMBDA		55
Vertical tail sweep	LAMBDAvt		65
Fuselage structural length	**L**	ft	**157,2496**
Electrical routing distance, generators to avionics to cockpit	**La**	ft	94,34975
Duct length	**Ld**	ft	47,17488
Length from engine front to cockpit	**Lec**	ft	62,89984
Length of main landing gear	**Lm**	in	113,2197
Nose gear length	**Ln**	in	150,9596
Single duct length (see Fig)	**Ls**	??	23,58744
Length of engine shroud	**Lsh**	ft	9,434975
Tail length; wing 1/4 to tail 1/4	Lt	ft	78,62479
Length of tailpipe	Ltp	ft	2
Mach number	M		2
Number of crew	Nc		2
1 single pilot; 1.2 pilot+backseater; 2.0 pilot+copassenger	Nci		1,2
Number of engines	Nen		4
Number of generators	Ngen		4
Ultimate Landing Load Factor: Ngear*1.5	Nl		4,5
Number of nose wheels	Nnw		2
Number of flight control systems	Ns		3
Number of fuel tanks	Nt		2
Number of hydraulic utility functions	Nu		2
Ultimate load factor = 1.5*limit load factor	Nz		6
System electrical rating	Rkva		5
Total area of control surfaces	**Scs**	ft2	152,8462
Control surface area (wing mounted)	**Scsw**	ft2	152,8462
Specific Fuel Consumption at maximum thrust	SFC		1,2
Firewall surface area	Sfw	ft2	80
Horizontal tail area	Sht	ft2	0
Rudder area	**Sr**	ft2	76,42308
Vertical tail area	**Svt**	ft2	152,8462
Trapezoidal Wing Area	**Sw**	ft2	**1528,462**
Thickness ratio	t/c		0,03
Total engine thrust	**T**	lb	**10018,75**
Thrust per engine	**Te**	lb	2504,688
Integral tanks volume	**Vi**	gal	5794,897
Self-sealing "protected" tanks volume	**Vp**	gal	2897,448
Total fuel volume	**Vt**	gal	4829,081
Fuselage structural width	W	ft	10
Design gross weight	**Wdg**	lb	80150
Engine weight, each	**Wen**	lb	**1290,576**
Fuel weight	**Wf**	lb	34238,18
Landing design gross weight	**Wl**	lb	45911,82
Uninstalled avionics weight	Wuav	lb	1000

Wing	9899,397421		
Horizontal Tail	0		
Vertical Tail	239,3478982		
Fuselage	1335,339431		
Cabin pressure	2000		
Main Landing Gear	2124,46889		
Nose Landing Gear	614,9798103		
Engine Mounts	48,66349933		
Firewall	90,4		
Engine Section	40,79840232		
Air Induction System	8182,030033		
Tailpipe	140		
Engine Cooling	858,5827593		
Oil Cooling	156,1812504		
Engine Controls	106,5040105		
Starter	25,97023618		
Fuel System and Tanks	1245,248975		
Flight Controls	790,3661453		
Instruments	194,3162664		
Hydraulics	58,98980402		
Electrical	421,3481813		
Avionics	1332,664589		
Furnishings	543,2		
Air Conditioning and Anti-Ice	258,1633774		
Handling Gear	25,648		
Lavatories	17,63732272		
			W/Wtotal
Wempty	**30750,2463**	0,383655	
Wgross first estimate	**80150**		
Swing	1528,461585 ft2		
Wfuel	**34238,1811**	0,427172	
Wpayload	10000	0,124765	
Wengines	**5162,305399**	0,064407	
Wtotal	**80150,73**	1	
Swing	1528,47556 ft2		
Altitude	***55000*** ft		
W/S(Z)	***52,438348*** lb/ft2		
Speed(Z)	***590,614*** m/s		
T/Weng(Z)	***1,9407511***		
Wf/W0(Z)	***0,4271763***		

Appendices #5: Weight model results for cruise altitude Z=60,000ft

Span	***B***	***ft***	***79,875018***
Aspect ratio	***A***		***2,67***
Aspect ratio vertical tail	Avt		0,8
Horizontal tail span	Bh	ft	0
Fuselage structural depth	D	ft	0,656
Engine diameter	De	ft	5
Fuselage width at horizontal tail intersection	Fw	ft	0
0 for conventional tail, 1 for "T" tail	Ht/Hv		0
2.25 for cross-beam gear; 1 otherwise	Kcb		1
Duct constant (see Fig)	Kd		1
0.768 for delta wing; 1 otherwise	Kdw		0,768
0.774 for delta wing aircraft; 1 otherwise	Kdwf		0,774
1.45 if mission completion required after failure	Kmc		1
1.047 for rolling tail; 1 otherwise	Krht		1
0.826 for tripod gear; 1 otherwise	Ktpg		1
1.62 for variable geometry; 1 otherwise	Kvg		1
1.19 for variable sweep wing; 1 otherwise	Kvs		1
1.425 if variable sweep wing; 1 otherwise	Kvsh		1
Wing sweep at 25% MAC	LAMBDA		55
Vertical tail sweep	LAMBDAvt		65
Fuselage structural length	**L**	ft	**196,6154287**
Electrical routing distance, generators to avionics to cockpit	**La**	ft	117,9692572
Duct length	**Ld**	ft	58,98462862
Length from engine front to cockpit	**Lec**	ft	78,6461715
Length of main landing gear	**Lm**	in	141,5631087
Nose gear length	**Ln**	in	188,7508116
Single duct length (see Fig)	**Ls**	??	29,49231431
Length of engine shroud	**Lsh**	ft	11,79692572
Tail length; wing 1/4 to tail 1/4	Lt	ft	98,30771437
Length of tailpipe	Ltp	ft	2
Mach number	M		2
Number of crew	Nc		2
1 single pilot; 1.2 pilot+backseater; 2.0 pilot+copassenger	Nci		1,2
Number of engines	Nen		4
Number of generators	Ngen		4
Ultimate Landing Load Factor: Ngear*1.5	Nl		4,5
Number of nose wheels	Nnw		2
Number of flight control systems	Ns		3
Number of fuel tanks	Nt		2
Number of hydraulic utility functions	Nu		2
Ultimate load factor = 1.5*limit load factor	Nz		6
System electrical rating	Rkva		5
Total area of control surfaces	**Scs**	ft2	238,9520033
Control surface area (wing mounted)	**Scsw**	ft2	238,9520033
Specific Fuel Consumption at maximum thrust	SFC		1,2
Firewall surface area	Sfw	ft2	80
Horizontal tail area	Sht	ft2	0
Rudder area	**Sr**	ft2	119,4760017
Vertical tail area	**Svt**	ft2	238,9520033
Trapezoidal Wing Area	**Sw**	ft2	**2389,520033**
Thickness ratio	t/c		0,03
Total engine thrust	**T**	lb	**12355**
Thrust per engine	**Te**	lb	3088,75
Integral tanks volume	**Vi**	gal	7146,195707
Self-sealing "protected" tanks volume	**Vp**	gal	3573,097854
Total fuel volume	**Vt**	gal	5955,16309
Fuselage structural width	W	ft	10
Design gross weight	**Wdg**	lb	98840
Engine weight, each	**Wen**	lb	**1992,741935**
Fuel weight	**Wf**	lb	42222,1063
Landing design gross weight	**Wl**	lb	56617,8937
Uninstalled avionics weight	Wuav	lb	1000

Wing	14777,07694		
Horizontal Tail	0		
Vertical Tail	292,251072		
Fuselage	1606,815209		
Cabin pressure	2000		
Main Landing Gear	2782,377125		
Nose Landing Gear	730,7576425		
Engine Mounts	54,94260514		
Firewall	90,4		
Engine Section	55,7080109		
Air Induction System	9446,047406		
Tailpipe	140		
Engine Cooling	1073,520241		
Oil Cooling	156,1812504		
Engine Controls	111,9196116		
Starter	30,45496459		
Fuel System and Tanks	1447,792075		
Flight Controls	983,380938		
Instruments	194,3162664		
Hydraulics	58,98980402		
Electrical	430,8676927		
Avionics	1332,664589		
Furnishings	543,2		
Air Conditioning and Anti-Ice	258,1633774		
Handling Gear	31,6288		
Lavatories	17,63732272		
			W/Wtotal
Wempty	**38647,09295**	0,39101	
Wgross first estimate	**98840**		
Swing	2389,520033	ft2	
Wfuel	**42222,1063**	0,42718	
Wpayload	10000	0,10117	
Wengines	**7970,967742**	0,08065	
Wtotal	**98840,167**	1	
Swing	2389,52407	ft2	
Altitude	***60000***	ft	
W/S(Z)	***41,3639554***	lb/ft2	
Speed(Z)	***590,614004***	m/s	
T/Weng(Z)	***1,55***		
Wf/W0(Z)	***0,42717631***		

Appendices #6: Weight model results for cruise altitude Z=65,000ft

Span	***Bh***	***ft***	***105,568***
Aspect ratio	***A***		***2,67***
Aspect ratio vertical tail	Avt		0,8
Horizontal tail span	Bh	ft	0
Fuselage structural depth	D	ft	0,656
Engine diameter	De	ft	5
Fuselage width at horizontal tail intersection	Fw	ft	0
0 for conventional tail, 1 for "T" tail	Ht/Hv		0
2.25 for cross-beam gear; 1 otherwise	Kcb		1
Duct constant (see Fig)	Kd		1
0.768 for delta wing; 1 otherwise	Kdw		0,768
0.774 for delta wing aircraft; 1 otherwise	Kdwf		0,774
1.45 if mission completion required after failure	Kmc		1
1.047 for rolling tail; 1 otherwise	Krht		1
0.826 for tripod gear; 1 otherwise	Ktpg		1
1.62 for variable geometry; 1 otherwise	Kvg		1
1.19 for variable sweep wing; 1 otherwise	Kvs		1
1.425 if variable sweep wing; 1 otherwise	Kvsh		1
Wing sweep at 25% MAC	LAMBDA		55
Vertical tail sweep	LAMBDAvt		65
Fuselage structural length	**L**	ft	**259,8594**
Electrical routing distance, generators to avionics to cockpit	**La**	ft	155,9156
Duct length	**Ld**	ft	77,95781
Length from engine front to cockpit	**Lec**	ft	103,9437
Length of main landing gear	**Lm**	in	187,0987
Nose gear length	**Ln**	in	249,465
Single duct length (see Fig)	**Ls**	??	38,9789
Length of engine shroud	**Lsh**	ft	15,59156
Tail length; wing 1/4 to tail 1/4	Lt	ft	129,9297
Length of tailpipe	Ltp	ft	2
Mach number	M		2
Number of crew	Nc		2
1 single pilot; 1.2 pilot+backseater; 2.0 pilot+copassenger	Nci		1,2
Number of engines	Nen		4
Number of generators	Ngen		4
Ultimate Landing Load Factor: Ngear*1.5	Nl		4,5
Number of nose wheels	Nnw		2
Number of flight control systems	Ns		3
Number of fuel tanks	Nt		2
Number of hydraulic utility functions	Nu		2
Ultimate load factor = 1.5*limit load factor	Nz		6
System electrical rating	Rkva		5
Total area of control surfaces	**Scs**	ft2	417,3998
Control surface area (wing mounted)	**Scsw**	ft2	417,3998
Specific Fuel Consumption at maximum thrust	SFC		1,2
Firewall surface area	Sfw	ft2	80
Horizontal tail area	Sht	ft2	0
Rudder area	**Sr**	ft2	208,6999
Vertical tail area	**Svt**	ft2	417,3998
Trapezoidal Wing Area	**Sw**	ft2	**4173,998**
Thickness ratio	t/c		0,03
Total engine thrust	**T**	lb	**16875**
Thrust per engine	**Te**	lb	4218,75
Integral tanks volume	**Vi**	gal	9760,587
Self-sealing "protected" tanks volume	**Vp**	gal	4880,294
Total fuel volume	**Vt**	gal	8133,823
Fuselage structural width	W	ft	10
Design gross weight	**Wdg**	lb	135000
Engine weight, each	**Wen**	lb	**3407,927**
Fuel weight	**Wf**	lb	57668,8
Landing design gross weight	**Wl**	lb	77331,2
Uninstalled avionics weight	Wuav	lb	1000

Wing	24983,48128		
Horizontal Tail	0		
Vertical Tail	384,2735332		
Fuselage	2060,234623		
Cabin pressure	2000		
Main Landing Gear	3945,633701		
Nose Landing Gear	919,6023065		
Engine Mounts	65,81220552		
Firewall	90,4		
Engine Section	81,84774974		
Air Induction System	11301,36178		
Tailpipe	140		
Engine Cooling	1418,832116		
Oil Cooling	156,1812504		
Engine Controls	119,0679855		
Starter	38,59782946		
Fuel System and Tanks	1811,588424		
Flight Controls	1291,748309		
Instruments	194,3162664		
Hydraulics	58,98980402		
Electrical	443,0533334		
Avionics	1332,664589		
Furnishings	543,2		
Air Conditioning and Anti-Ice	258,1633774		
Handling Gear	43,2		
Lavatories	17,63732272		
			W/Wtotal
Wempty	**53699,88779**	0,397776	
Wgross first estimate	**135000**		
Swing	4173,997861 ft2		
Wfuel	**57668,80161**	0,427175	
Wpayload	10000	0,074074	
Wengines	**13631,70664**	0,100975	
Wtotal	**135000,4**	1	
Swing	4174,010106 ft2		
Altitude	***65000*** ft		
W/S(Z)	***32,343093*** lb/ft2		
Speed(Z)	***590,614*** m/s		
T/Weng(Z)	***1,2379228***		
Wf/W0(Z)	***0,4271763***		

Appendices #7: Weight model results for cruise altitude Z=70,000ft

Span	***Bh***	***ft***	***153,614***
Aspect ratio	***A***		***2,67***
Aspect ratio vertical tail	Avt		0,8
Horizontal tail span	Bh	ft	0
Fuselage structural depth	D	ft	0,656
Engine diameter	De	ft	5
Fuselage width at horizontal tail intersection	Fw	ft	0
0 for conventional tail, 1 for "T" tail	Ht/Hv		0
2.25 for cross-beam gear; 1 otherwise	Kcb		1
Duct constant (see Fig)	Kd		1
0.768 for delta wing; 1 otherwise	Kdw		0,768
0.774 for delta wing aircraft; 1 otherwise	Kdwf		0,774
1.45 if mission completion required after failure	Kmc		1
1.047 for rolling tail; 1 otherwise	Krht		1
0.826 for tripod gear; 1 otherwise	Ktpg		1
1.62 for variable geometry; 1 otherwise	Kvg		1
1.19 for variable sweep wing; 1 otherwise	Kvs		1
1.425 if variable sweep wing; 1 otherwise	Kvsh		1
Wing sweep at 25% MAC	LAMBDA		55
Vertical tail sweep	LAMBDAvt		65
Fuselage structural length	**L**	ft	**378,127**
Electrical routing distance, generators to avionics to cockpit	**La**	ft	226,8762
Duct length	**Ld**	ft	113,4381
Length from engine front to cockpit	**Lec**	ft	151,2508
Length of main landing gear	**Lm**	in	272,2514
Nose gear length	**Ln**	in	363,0019
Single duct length (see Fig)	**Ls**	??	56,71905
Length of engine shroud	**Lsh**	ft	22,68762
Tail length; wing 1/4 to tail 1/4	Lt	ft	189,0635
Length of tailpipe	Ltp	ft	2
Mach number	M		2
Number of crew	Nc		2
1 single pilot; 1.2 pilot+backseater; 2.0 pilot+copassenger	Nci		1,2
Number of engines	Nen		4
Number of generators	Ngen		4
Ultimate Landing Load Factor: Ngear*1.5	Nl		4,5
Number of nose wheels	Nnw		2
Number of flight control systems	Ns		3
Number of fuel tanks	Nt		2
Number of hydraulic utility functions	Nu		2
Ultimate load factor = 1.5*limit load factor	Nz		6
System electrical rating	Rkva		5
Total area of control surfaces	**Scs**	ft2	883,7936
Control surface area (wing mounted)	**Scsw**	ft2	883,7936
Specific Fuel Consumption at maximum thrust	SFC		1,2
Firewall surface area	Sfw	ft2	80
Horizontal tail area	Sht	ft2	0
Rudder area	**Sr**	ft2	441,8968
Vertical tail area	**Svt**	ft2	883,7936
Trapezoidal Wing Area	**Sw**	ft2	**8837,936**
Thickness ratio	t/c		0,03
Total engine thrust	**T**	lb	**28337,5**
Thrust per engine	**Te**	lb	7084,375
Integral tanks volume	**Vi**	gal	16390,56
Self-sealing "protected" tanks volume	**Vp**	gal	8195,278
Total fuel volume	**Vt**	gal	13658,8
Fuselage structural width	W	ft	10
Design gross weight	**Wdg**	lb	226700
Engine weight, each	**Wen**	lb	**7165,494**
Fuel weight	**Wf**	lb	96840,87
Landing design gross weight	**Wl**	lb	129859,1
Uninstalled avionics weight	Wuav	lb	1000

Wing	53197,41326		
Horizontal Tail	0		
Vertical Tail	582,803344		
Fuselage	2979,597141		
Cabin pressure	2000		
Main Landing Gear	6469,894961		
Nose Landing Gear	1289,240246		
Engine Mounts	88,84840248		
Firewall	90,4		
Engine Section	139,4513502		
Air Induction System	14383,8463		
Tailpipe	140		
Engine Cooling	2064,573361		
Oil Cooling	156,1812504		
Engine Controls	129,4072632		
Starter	57,23377267		
Fuel System and Tanks	2629,778681		
Flight Controls	1864,203959		
Instruments	194,3162664		
Hydraulics	58,98980402		
Electrical	459,9874039		
Avionics	1332,664589		
Furnishings	543,2		
Air Conditioning and Anti-Ice	258,1633774		
Handling Gear	72,544		
Lavatories	17,63732272		
			W/Wtotal
Wempty	**91200,37605**	0,40229	
Wgross first estimate	**226700**		
Swing	8837,935752 ft2		
Wfuel	**96840,86907**	0,42717	
Wpayload	10000	0,044111	
Wengines	**28661,97618**	0,12643	
Wtotal	**226703,2**	1	
Swing	8838,061336 ft2		
Altitude	***70000*** ft		
W/S(Z)	***25,650786*** lb/ft2		
Speed(Z)	***590,614*** m/s		
T/Weng(Z)	***0,9886792***		
Wf/W0(Z)	***0,4271763***		

Appendices #8: From Design Parameters to Sonic Boom Optimization

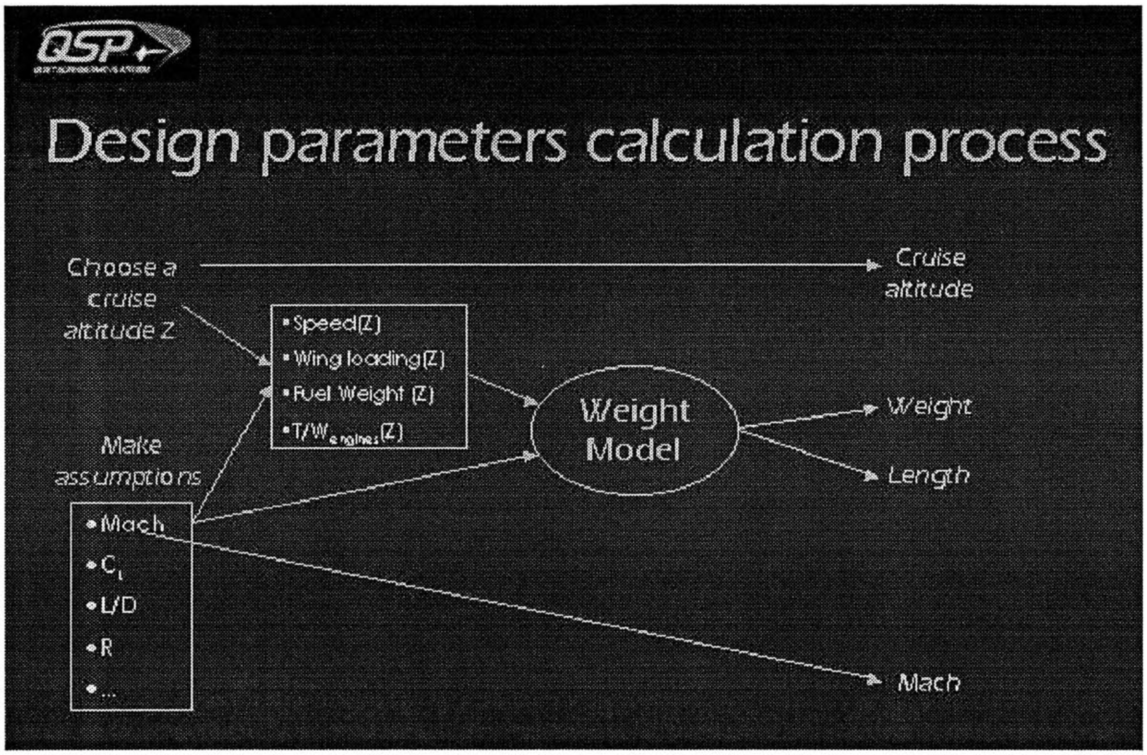

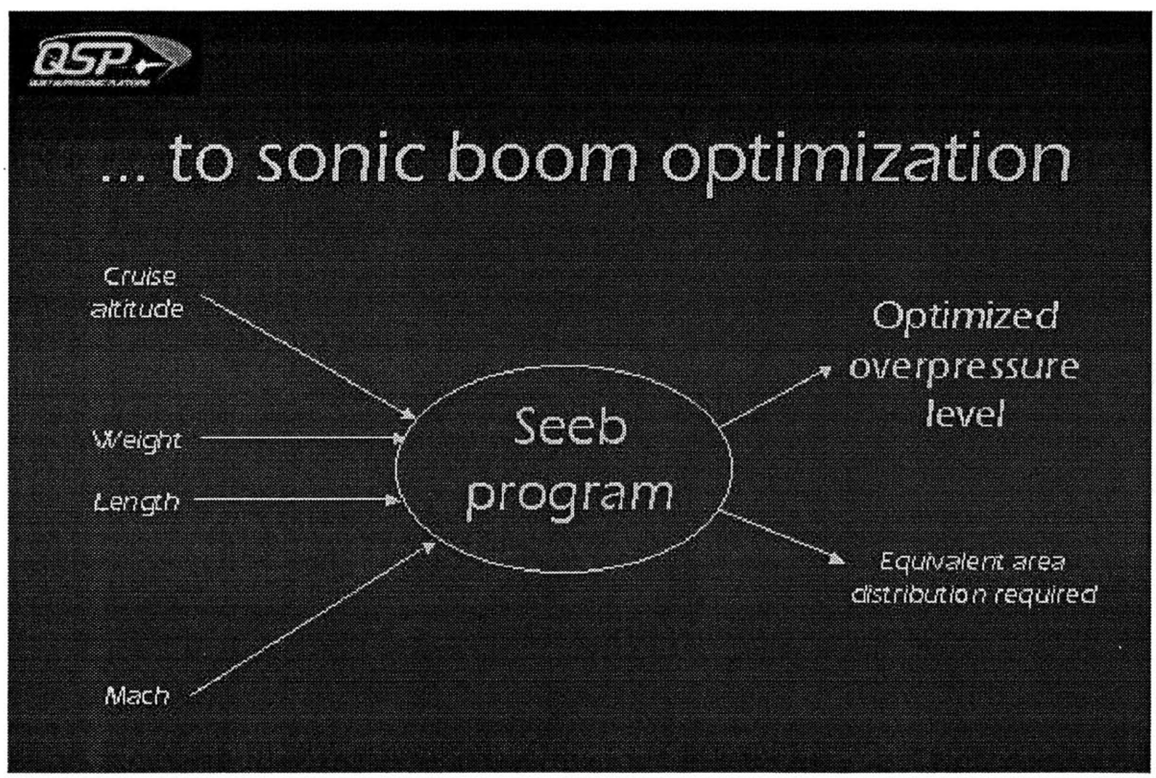

Appendices #9: Proposed Configuration